Isothermal titration calorimetry

Margarida Bastos[1,7], Olga Abian[2,3,4,7], Christopher M. Johnson[5], Frederico Ferreira-da-Silva[6], Sonia Vega[2], Ana Jimenez-Alesanco[2], David Ortega-Alarcon[2] and Adrian Velazquez-Campoy[2,3,4,†]

[1] CIQUP, Institute of Molecular Sciences (IMS), Department of Chemistry and Biochemistry, Faculty of Sciences, University of Porto, Porto, Portugal

[2] Institute of Biocomputation and Physics of Complex Systems (BIFI), and Department of Biochemistry and Molecular and Cell Biology, University of Zaragoza, Zaragoza, Spain

[3] Aragon Institute for Health Research (IIS Aragon), Zaragoza, Spain

[4] Biomedical Research Networking Center in Hepatic and Digestive Diseases (CIBERehd), Madrid, Spain

[5] MRC Laboratory of Molecular Biology, Cambridge, UK

[6] Instituto de Biologia Molecular e Celular (IBMC) and Instituto de Investigação e Inovação em Saúde (i3S), Universidade do Porto, Porto, Portugal

[7] These authors contributed equally: Margarida Bastos, Olga Abian

[†] email: adrianvc@unizar.es

Abstract

Isothermal titration calorimetry (ITC) has become the gold-standard for studying molecular interactions in solution. Although it is increasingly being used in the soft matter and synthetic chemistry fields, ITC is most widely used for characterizing molecular interactions between ligands and macromolecules. This Primer starts by presenting the technique's foundations and instrumentation, including a brief description of the standard assay, followed by a review of common applications. Further extensions and modifications of the technique are explored. These adaptations enable key features to be studied, such as cooperative effects associated with complex biological interactions and their regulation, alongside applications to other fields, including partition to membranes, kinetics and soft matter. Advantages and caveats in ITC are discussed, with a focus on best practices, instrument calibration, experimental design, data analysis and data reporting, as well as recent and future developments.

Introduction

Calorimetry is an experimental technique that measures the heat associated with a process to follow and quantify that process. Biocalorimetry is a recent application that uses calorimetry to measure heat for processes involving biological molecules. Most biological binding processes involve molecular interactions that are mediated by noncovalent forces, such as hydrogen bonds

and van der Waals interactions, which represent a special type of reversible chemical reaction or process. Heat is a process function, which means the heat in a given process will depend on the constraints under which the process is studied. Isothermal titration calorimetry (ITC) measurements are performed at constant temperature (T) using a thermostat and at constant pressure (P) with a barostat. Under these constraints, the process is isothermal and isobaric meaning the associated heat will be equal to the change in enthalpy in the system (ΔH). The Gibbs energy is the thermodynamic potential that governs the equilibrium in a system, and its change (ΔG) determines the feasibility, or spontaneity, of a given process at constant T and P. The change in entropy (ΔS) reflects changes in degrees of freedom associated with desolvation, conformational, vibrational and roto-translational changes. The equilibrium constant (K_{eq}) determines the system composition at equilibrium and quantifies the tendency to form the end products, for example complex formation in a binding process. It is related to the standard Gibbs energy of the process by $\Delta G^0 = -RT \ln K_{eq}$. The affinity of a given interaction may be quantified using the equilibrium association (K_a) and dissociation (K_d) constants and the Gibbs energy of binding. A more negative Gibbs energy indicates higher affinity and greater intermolecular complex stability. Partitioning the Gibbs energy into enthalpic and entropic contributions provides additional information about the driving forces of binding.

During an ITC assay, a titration — step-wise mixing of one reactant into another reactant — is performed at constant T and P, while measuring the heat associated with the binding reaction[1,2]. The equipment measures the heat released or absorbed after each reactant addition. ITC is the only technique that can directly and simultaneously determine ΔH^0 and K_{eq} (either as K_a or K_d, where $K_a = 1/ K_d$) for a binding process (**Box 1**). Using well-known relationships, other fundamental quantities can be readily calculated, such as ΔG^0 and ΔS^0. All parameters are defined in the standard state, with all reactant concentrations of 1 M and 1 atmosphere pressure (1 atm ≈ 0.1 MPa), at the defined temperature (for example, 298.15 K). The biochemical standard state is additionally defined at pH 7, equivalent to a proton concentration of 0.1 μM.

Performing experiments at different temperatures enables the heat capacity change upon binding (ΔC_P) to be obtained. ΔC_P reflects changes in the desolvation of reactants, with a major contribution from desolvation of non-polar molecular surfaces[3]. A large ΔC_P is a fundamental property in hydrophobic interactions. Consequently, using ITC at different temperatures is a straightforward way to assess the importance of the hydrophobic effect on a binding process[4]. Other variables that can be obtained by ITC include the stoichiometry, which defines the relationship between the number of molecules interacting to form the complex. However, uncertainties in reactant concentrations can obscure the stoichiometry calculation (see section **Experimentation**). When reporting results from ITC, the International System of Units promotes the joule (J) as the unit for heat. Traditionally, calorimetrists have used the calorie (1 calorie = 4.184 J). ITC results are reported using both units.

All high-sensitivity ITC instruments have a dual or twin cell design. This setup consists of two virtually identical cells: the sample cell, where the solution of one reactant is placed, and the reference cell, which contains a buffer or water. The other reactant solution is placed in the syringe and small aliquots are delivered to the sample cell during the titration experiment (**Figure 1**). To study interactions between biological molecules, dilute solutions are often required to overcome limitations in reactant availability, purity, solubility, aggregation propensity and to avoid non-idealities. The total heat corresponding to the binding reaction and saturation of the reactant in the sample cell is distributed over several injections, and decreases towards saturation. As an example, in a typical ITC assay with a cell volume of 200 μL, injected volume of 2 μL, titrand cell concentration of 10 μM, titrant syringe concentration of 100 μM and binding enthalpy of 20 kJ/mol, the first injection has an associated heat effect <4 μJ, and the cumulative heat effect after 20 injections is <40 μJ. The observed change in measured thermal power may be <0.5 μJ/s. This type of limitations drove the development of high-sensitivity ITC instruments that could be used with these amounts of biological samples.

Advances in technology, electronics and commercialization, mean calorimetry is no longer a technique for specialized labs using home-built instruments. Small amounts of heat can be detected, referred to as microcalorimetry. All available instruments offer automatic titration in computer-controlled experiments, in parallel with automatic data collection. Sample loading and instrument cleaning can be done manually, but newer models have a semi-automated maintenance set and scripts to automate cleaning and minimize operator intervention (see **Supplementary Information,** sections **Details of present instruments on the market** and **Sensitivity of current ITC instruments**). Full automation has increased experimental throughput, which was considered low in biocalorimetry compared to biological standards. The output of current calorimetric instruments can be expanded with an automatic sampling unit and robotic elements for unattended operation. Automated instruments include cleaning and sample loading between programmed experiments and can produce data as accurate for determining thermodynamic parameters as manual ITCs.

The molecule placed in the injecting syringe is referred to as the titrant (injection volume, v), while the molecule in the sample cell is called the titrand (cell volume, V_0). However, the situation should be completely symmetric and reverse titrations, which exchange titrant and titrand locations, can also be performed. Reverse titrations are recommended where materials allow, to assess self-association of the interacting molecules or other concentration-dependent phenomena, as well as to test the robustness of the binding model. Although the binding equilibrium is the same for direct and reverse titrations, the path through equilibrium states and accessible ligation states are different when one of the interacting molecules has more than one binding site for the other molecule. Injecting a ligand into a macromolecule is not the same as injecting a macromolecule into a ligand. In terms of ligation states and their interconversion, direct titration offers better resolution and more intuitive interpretation. Recombinant protein technology provides a sufficient amount of protein sample to enable the selection of titrant based on availability, solubility, tendency to aggregate at high concentrations, ability to undergo self-association-related processes and binding stoichiometry. These choices rely on the much higher titrant concentration in the syringe than titrand concentration in the cell. In addition, if a molecule has several binding sites for the other molecule, it is more convenient to place the former in the cell.

Any binding process may be accompanied by a plethora of other potential equilibria. For example, the interaction between two proteins may occur simultaneously with conformational changes, proton uptake at or release from ionizable sidechains, or ion release from the binding interface. If one experiment is performed under a single set of experimental conditions, all binding parameters that are estimated and used to characterize the interaction must be considered as apparent binding parameters. This is because they contain a contribution from the interaction event and other simultaneous equilibria that were measured concomitantly. ITC measures the total heat exchange, which encompasses all processes involved in the interaction. Unless additional experiments are performed to disentangle the contributions, it cannot be concluded whether any additional equilibria, for example proton ionization changes, contribute to the observed binding parameters.

The binding parameters are traditionally interpreted by considering the different non-covalent intermolecular interactions established between binding partners. However, two given molecules do not interact in a vacuum, but normally in an aqueous based buffer. Water is a polar solvent with an extensive network of hydrogen bonds. Water molecules can interact with the two interacting molecules. The complex may be formed by breaking interactions between water molecules, or between water molecules and the reacting molecules. The binding parameters are the net result of many interactions breaking and forming[5-8]. Two interacting molecules in solution must undergo partial desolvation to interact. This desolvation contributes unfavorably to the enthalpy, as $\Delta H > 0$ from the rupture of hydrogen bonds, electrostatic and van der Waals interactions with water molecules, but favorably to the entropy, as $-T\Delta S < 0$ from the increased mobility of released water molecules. The formation of non-covalent bonds between both

interacting molecules — hydrogen bonds, electrostatic, van der Waals and hydrophobic interactions — contributes favorably to the enthalpy, as $\Delta H < 0$ from the formation of intermolecular interactions, but unfavorably the entropy, as $-T\Delta S > 0$ from conformational changes, reduced roto-translational degrees of freedom and restricted mobility degrees of freedom. Other components, such as ions bound to the reactants or complex, may additionally contribute to the overall binding parameters if they are exchanged with the bulk solvent on complex formation. However, this description of the overall enthalpy and entropy changes is simplistic and there is controversy about the general validity and usefulness of this interpretation of the binding parameters[9-11]. Nevertheless, it serves as starting point to understand and discuss the obtained thermodynamic parameters.

Parameters determined by ITC help to describe and interpret biological interactions, enabling further conclusions to be drawn. As an example, ferrochelatase is the terminal enzyme of the heme biosynthetic pathway and catalyzes the chelation of Fe(II) into the protoporphyrin IX ring. ITC was used to determine the interaction of ferrochelatase with mesoporphyrin, which revealed a stoichiometry of one mesoporphyrin molecule bound per protein monomer[12]. This binding occurs through a strongly exothermic interaction ($\Delta H^0 = -97.1$ kJ/mol) associated with the uptake of two protons from the buffered solution. From the results, it could be inferred that hydrogen bonding between ferrochelatase and mesoporphyrin is a key factor in the interaction. Another example is the comparison of the thermodynamic binding parameters from tripeptide and second-generation inhibitors interacting with the HIV-1 protease to those from first-generation clinical inhibitors[13-16]. This gives strong evidence for a different mode of interaction, even when inhibitor binding is occurring at the same binding site. Second-generation inhibitors, which are less susceptible to resistance mutations in the protein target, show enthalpically driven binding, while first-generation inhibitors show entropically driven binding. These thermodynamic profiles correlate with structural features. Second-generation inhibitors are quite polar and moderately conformationally flexible. By contrast, first-generation inhibitors are very hydrophobic and conformationally constrained. As another example, the interaction of DNA with intercalators and groove binders show completely different energetic signatures: enthalpically driven for intercalators and entropically driven for groove binders[17]. Similarly, protein binding to the DNA major groove is an enthalpically driven process, whereas binding to the minor groove is an entropically driven process[18].

The set of thermodynamic parameters for a given binding interaction (ΔG^0, ΔH^0, ΔS^0, and ΔC_P) constitutes the thermodynamic binding profile or thermodynamic signature. Because the entropy unit is J K^{-1} mol^{-1} or cal K^{-1} mol^{-1}, to visualize and compare binding profiles, the entropic contribution $-T\Delta S^0$, rather than ΔS^0 is often used. Because ΔG^0 must be negative for binding to occur, any negative term from ΔH^0 and $-T\Delta S^0$ would favor binding, while any positive term would oppose binding. Careful interpretation of these parameters is needed because calorimetry results reflect all molecular processes taking place. Even when sufficient experiments have been done to remove or rule out additional contributions, the thermodynamic profile still reflects an enormous number of intermolecular interactions forming and breaking upon complex formation. However, this should not discourage the use of calorimetry and thermodynamics, as several perspectives can be adopted. It is possible to compare profiles from similar or dissimilar molecules interacting with a common binding partner, to provide insightful results for binding affinity, specificity, selectivity, and cooperativity[19-24]. Similarly, comparing profiles for variants of a given molecule — for example, protein mutants associated with pathologies compared to the wild type version — interacting with a common molecule may indicate significant differences and provide information about the molecular basis of a disease or the pathogenic role of certain mutations in a given protein. Whenever possible, this information should be interpreted together with structural data to obtain structural and functional implications. All these ideas may be expanded to different applications in biomedicine and biotechnology, but are beyond the scope of this Primer. Here, the aim is to provide a short, introductory overview of ITC, addressing the main aspects of the technique in a precise and detailed way, together with hints on how to handle the

data and interpret the estimated thermodynamic parameters within the biological context of the studied problem.

The main advantages and disadvantages of ITC are summarized in **Table 1**. Some of these disadvantages were applicable to earlier instruments, but have been addressed by recent developments. Current instruments are largely automated and the calorimetric cells are isolated from the laboratory environment. An experiment can be performed in less than 1 hour. Unattended operation in fully automated versions enables a throughput of about 20 experiments per day. More dilute solutions can now be studied, meaning common problems, such as protein aggregation, are reduced and experiments can be conducted with much less than a mg of medium-sized protein. While this may be more than the quantity required for most spectroscopic techniques, it is comparable to other methods, for instance nuclear magnetic resonance spectroscopy. Analysis of ITC data may appear complicated because, unlike other binding techniques, no approximations are made, such as neglecting ligand depletion due to binding; no linearization transformations are performed, such as Scatchard plots; and the binding equilibrium is exactly solved using nonlinear least-squares (NLLS) fitting analysis. Fortunately, manufacturer-supplied software and online applications make analysis straightforward, although they must be used appropriately and with an element of critical thinking. ITC, like any other binding technique, has a window of binding affinity over which the K_a or K_d can be reliably determined. This is based on the amount of titrand in the cell. However, ITC is uniquely placed to perform displacement binding experiments that can extend the practical range for affinity determination by several orders of magnitude.

Experimentation

Instrument set-up

Reaction heat is the monitoring probe for the calorimetric titration, equivalent to the indicator dye in a redox or acid-based titration. It provides useful information, such as the enthalpy change in a direct manner, or the equilibrium constant and Gibbs energy change in an indirect manner.

ITC instruments used to study biochemical and biological systems operate as power meters. They have an actuator element, a resistor, that communicates a constant, small thermal power to the reference cell and a feedback actuator element, another resistor, that provides variable thermal power to the sample cell depending on the temperature difference between the cells (see **Supplementary Information,** sections **Details of present instruments on the market**, **Sensitivity of current ITC instruments** and **Data collection and output files in present instruments)**. They operate according to the dynamic power compensation principle. Any temperature difference is promptly cancelled by an opposing modulation of the thermal power applied to the sample cell. The power is either increased or decreased compared to the constant reference thermal power. The recorded measurement is the thermal power (μW or μJ/s, or μcal/s) that the feedback actuator provides to the sample cell to keep the temperature difference as small as possible ($\Delta T \approx 0$). For a given injection of titrant, a deflection from the baseline instantaneous differential power, dP, in the form of an upward or downward peak is observed. Peak direction (up or down) for an exothermic reaction, with the opposite for an endothermic reaction, depends on the settings in the data collection software. For a complete assay, a series of peaks will be obtained, which constitutes a thermogram, a plot of thermal power as a function of time (**Figure 2**). Time integration of each peak from the baseline provides the heat associated with each injection, which contains the contribution from the reaction, but also other non-reaction related contributions. Plotting the heats derived from peak integration as a function of the reaction progress gives the binding isotherm. Any changes in the experimental instrumental settings or conditions may change the appearance of the thermogram and the binding isotherm.

In heat compensation calorimeters the feedback gain can be set to zero and the calorimeter acts in passive heat conduction mode. With zero feedback heat is dissipated passively, without active compensation. This results in larger instrumental time constants and longer experimental run times. However, the passive mode implies a better power detection limit, because the temperature perturbation after titrant addition is not actively compensated and the signal reaches higher transient values. The instrument thermal time constant is the time required to reach ~63% of a particular specified signal value. In a simplified manner, it is given by the quotient between the effective heat capacity and the effective thermal conductivity of the cell, together with the Peltier unit and the solution within the cell. Non-zero feedback results in reduced instrumental time constant — around 10 s in current instruments — with narrower injection peaks that are optimal for high throughput and labile biological samples only stable for a short time period. When the enthalpy of the reaction is very small, it is recommended to switch off the feedback, setting a zero-gain mode (see **Supplementary Information,** section **Dealing with overshooting**).

Thermal power traces for individual injections may be simple (**Figure 2b**) or multiphasic. Multiphasic injection traces reflect different contributions to the overall heat effect, with different magnitude and kinetics, resulting in complex shapes until all heat is evacuated from the cell and the signal returns to the baseline. In addition, binding isotherms may be simple (**Figure 2c**), which is typical for a single set of identical, independent binding sites in a protein, but may also be multiphasic, for example if there are two or more nonidentical or cooperative binding sites.

Equipment basics

Available ITC instruments are overflow type, which means the cells are completely filled and the operational volume for loading and running is greater than the calorimetrically sensed sample cell volume. This has two important implications. First, any injection of titrant into the sample cell is accompanied by the irreversible displacement of an equivalent volume from the sample cell to an external compartment. As there is no well-defined boundary between the reaction cell and expelled solution, the effective cell volume must be determined by chemical calibration. The volume given by the manufacturer is typically within 1%, unless the stirrer has been changed or modified. Second, the concentrations of various components before and after each injection into the measuring cell must be calculated based on assumptions about the composition of the expelled solution. These assumptions depend on the injection speed, mixing rate and locus of injection, where the needle is positioned inside the cell. Different software packages base their calculations on different assumptions. For example, assuming the expelled solution has the same composition as the solution before or during injection and mixing. This leads to slightly different concentrations and potentially different estimates of ΔH^0 and K_a. Any error in the assumption is compounded over the number of injections. To minimize uncertainty about the solution composition in the measuring cell after each injection for an overfilled reaction cell, the injection volume should be less than 1% of the measuring cell volume. Under these criteria different assumptions give similar results for the reactant concentrations.

To fully characterize an ITC instrument, it is important to know its basic parameters accurately. Users need to confirm the effective cell volume using a standard reaction; the injection volume by calibrating with water by weight or with a standard reaction; and the power sensitivity — the change in control heater power per change in input power — by using a standard reaction[25-27]. Calibration of the power sensitivity is often neglected, but it cannot be accurately assumed that the heat distribution and heat losses from the control heater are the same as the from a reaction inside the reaction vessel. These calibrations are a necessary part of the basic instrument characterization when using a new ITC, for maintenance, or if the syringe is changed. In addition,

users need to understand the effects of injection speed, working temperature, and stirring speed on the peak profiles in the thermogram.

Heat compensation calorimeters, based on the dynamic power compensation principle, allow the user to set the baseline reference power level depending on whether the reaction is expected to be exothermic or endothermic. This reference power triggers the feedback actuator on the sample cell (see **Supplementary Information,** section **Details of present instruments on the market**) and defines the position of the baseline. It also provides an important check for the quality of the experimental preparation, including previous cleaning. This is because the power signal where the ITC equilibrates prior to the first injection should be very close to the chosen reference power (in μW or μcal/s), or slightly lower due to the exothermic power generated by stirring.

Experimental design

A brief description of the basic settings is provided here as a general guide. A more detailed standard operation procedure can be found in a recent paper aimed at producing results that are precise, accurate and comparable[28]. Much effort has been devoted to minimizing uncertainties in the estimated binding parameters by optimizing experimental design[27,29-31]. Nevertheless, careful experimental design can be useless if it is not accompanied by thorough sample preparation and accurate data analysis.

When starting ITC measurements on a new system, any available information on binding affinity, stoichiometry and enthalpy are useful for setting up the experimental design. These values enable simulations of experimental data using software provided by the manufacturers. Without any design input, a guess of $K_a = 10^6\ M^{-1}$ and $\Delta H^0 = \pm 20$ kJ/mol is reasonable. The ideal ITC experiment will produce a binding isotherm that allows reliable and independent estimation of K_a and ΔH^0. Such a titration will have two plateau regions, at the start and end, joined by a sigmoidal change. The ΔH^0 will be roughly determined by the difference between the two plateaus, while K_a is related to the steepness of sigmoidal inflection. These estimates are independent and non-correlated since they arise from different geometric features of the curve[32]. It is not always possible to design experiments that give optimal data due to limitations imposed by the value of K_a or amount of available material. Non-sigmoidal binding isotherms are common and often unavoidable. These data will still yield K_a and ΔH^0 during the NLLS fitting, but there may be significant correlation between them[33,34].

When designing experiments, the *c* parameter is commonly used (where $c = n\,[\text{titrand}]_T\,K_a$ or $c = n\,[\text{titrand}]_T / K_d$, where *n* is the number of binding sites or the fraction of active titrand) to set the titrand cell concentration[35]. Although this is useful, it should be seen as a rough guide to help the initial choice of a good setup. It has been suggested that the success of an ITC binding process study is determined more by the total detectable heat, Q_T, and the maximal saturation or percentage of complex formed than by the *c* value magnitude[30].

At the end of an ITC titration sufficient saturation of the titrand must be achieved for good quality data. For this to happen, the final titrant concentration in the cell must be several times higher than that of the titrand (molar ratio ≥ 1). If a small total injected volume of titrant is required, the titrant concentration in the syringe must be considerably high. Consequently, the cell volume, total injected volume, and titrand concentration will determine the titrant concentration (see **Box 2**).

If the volume ratio v/V_0 is around 0.01 — close to the actual situation in current instruments — and the desired excess of titrant $[X]_T$ over titrand $[M]_T$ in the cell is more than double after 20 injections, then $[X]_0/[M]_0$ must be > 9 (see **Box 2**). The rule-of-thumb is to select a titrant concentration in the syringe 10–20x higher than the titrand. If no information is available about the interaction, a common set-up is to use 10–20 μM in the cell and 100–300 μM in the syringe.

When there is more than one binding site in the titrand or a low affinity, the multiplication factor must be increased to guarantee sufficient conversion of titrand to complex[29].

Sample preparation

Interacting molecules should be prepared in an appropriate buffer. For powder or lyophilized samples, this can be done by dissolution, while for liquid samples, buffers are prepared by dialysis, size exclusion chromatography or another solution exchange method. The composition of the buffer should maximize the physical and chemical stability of both titrant and titrand. Where possible, aggregation, degradation and unfolding should be avoided. Alongside the buffering system, reducing agents, such as DTT, TCEP or β-mercaptoethanol, may be required to avoid oxidation. Solubilizing agents of a different nature, for instance dimethyl sulfoxide, glycerol, amino acids or detergents, may be needed to promote solution stability for low-solubility hydrophobic compounds or aggregation-prone proteins. When these compounds need to be added, or if they are already present, for example in a protein after purification, special care must be taken when preparing the second reactant solution to ensure that all solvent solutions match and avoid buffer mismatches. To assess the possibility of a buffer mismatch, control dilution experiments must be performed. Control experiments should be undertaken in the same conditions as the binding experiments to evaluate whether significant dilution heat could be the result of buffer mismatch, for instance due to *pH* neutralization or solute dilution. With careful replicated measurements, it is often possible to subtract and remove this unspecific effect from the overall heat effect per injection. The final choice of buffer may often be a compromise between optimizing these conditions for measurement and their physiological relevance. Even the descriptor physiological condition ignores molecular crowding that occurs in vivo inside cells. However, it is generally desirable to obtain reliable estimates of binding parameters even under non-physiological conditions, rather than collecting data where no proper interaction has occurred, for example due to system aggregation, modification, or if additional chemical processes prevent interpretation.

Buffers can be involved in ionization events that are coupled to the interaction. As a result, the buffer is a major potential contributor to the measured binding energetics. If protons are exchanged between the complex and bulk solution upon binding, buffer ionization may contribute to the apparent enthalpy and entropy of binding. The larger the buffer ionization enthalpy, the larger the contribution. For example, the buffer TRIS has an ionization enthalpy of +47.45 kJ/mol, compared to buffer phosphate, which has an ionization enthalpy of +3.60 kJ/mol[36,37]:

$$\Delta H^0_{obs} = \Delta H^0 + \Delta n_{H^+} \Delta H^0_{B,ion} \quad (1)$$

where ΔH^0_{obs} is the directly observed enthalpy of binding; ΔH^0 is the intrinsic buffer-independent enthalpy of binding, which corresponds to the enthalpy of a titration performed using a buffer with zero ionization enthalpy, $\Delta H^0_{B,ion}$; and Δn_{H+} is the net number of exchanged protons upon complex formation between titrand and titrant molecules[38,39]. If this is the only concomitant effect, the parameters obtained after this correction will no longer be apparent binding parameters, but rather parameters that reflect the binding reaction (see **Figure 3**). The biologically relevant binding parameters will be those that include the ionization contribution of the functional groups involved in proton exchange, after removing the buffer influence.

It is sometimes suggested that some buffers are not good for ITC. However, as long as they do not interact specifically with any of the binding partners, all buffers are good for ITC. Importantly, buffers may help to amplify the apparent enthalpy to measurable values. According to (1), if the term $\Delta n_{H+}\Delta H^0_{B,ion}$ is significant, then proton exchange with the buffer will make ΔH^0_{obs} much different to ΔH^0. If ΔH^0 is close to zero, ΔH^0_{obs} would not be zero. However, if ΔH^0 and $\Delta n_{H+}\Delta H^0_{B,ion}$ cancel, ΔH^0_{obs} would be too small to detect the interaction. Understanding how the buffer might affect the estimated binding parameters, which can be assessed through experiments in different

buffers with similar pK_a and different $\Delta H^0_{B,ion}$, is key. This knowledge can be used to remove this unwanted, extrinsic contribution. Standard procedures and protocols are available to do this successfully[40-43].

Buffers should have a pK_a within 1 *pH* unit of the experimental *pH* and must not directly interact with the titrant or titrand. This is particularly important if metal ions are involved in the binding system. The buffer maintains the ionization state of the interacting molecules. When there are changes in ionization during binding, the buffer provides protons to, or receives protons from, the process. The ΔH^0 and ΔS^0 are affected by this additional coupled equilibrium, to an extent that depends on the enthalpy of buffer ionization (**Figure 3**). As the selected buffer has a pK_a close to the experimental *pH*, the binding affinity is not affected by buffer ionization. Polyprotic buffers with close pK_a values, for example citrate, should be avoided as it is difficult to remove the buffer ionization contribution from the binding enthalpy.

Ideally, the solutions of both interacting molecules should be prepared with an identical buffer, for example by dialyzing two proteins against the same buffer in the same beaker. The dialysis buffer may then be used to perform any additional sample dilutions required after concentration determination. When this is not possible, great care should be taken to match the solution conditions of titrant and titrand. Otherwise, the interaction heat may be masked by large mixing heats from the disparate solutions. This is particularly important when using dimethyl sulfoxide or glycerol, as they have significant heats of dilution.

The concentrations of the interacting molecules must be carefully determined as all estimated binding parameters — affinity, enthalpy and stoichiometry — are dependent on accurate concentrations. Low molecular weight compounds are usually dissolved after weighing. Concentrations can be analyzed if the compound is spectroscopically active or by using elemental analysis of nitrogen or sulphur. Otherwise, the weighed concentration must be used. Protein concentrations are normally determined from UV absorbance and a molar extinction coefficient[44]. If the experimentally determined extinction coefficient is not known, the estimated value can be derived from an empirical equation based on the protein sequence. For example, online resources such as ProtParam, which is available from the bioinformatics resource portal Expasy, provides fairly good results[45,46]. Proteins that contain additional cofactors or are labelled with extrinsic chromophores may also be quantified by absorbance at longer wavelengths. It is also possible to retain a sample of protein or peptide for amino acid analysis after ITC measurement. In this respect, it is useful to work with common stock solutions across multiple experiments as amino acid analysis is time consuming and costly. Colorimetric methods, such as the Bradford assay, should be avoided because they can suffer from large errors (up to 50%) depending on the similarity of the sample protein to the standard protein used.

All protein concentrations are subject to error if there is aggregated material present. Additionally, misfolding or contaminant proteins reduce the amount of active or binding competent protein. If possible, an orthogonal assay of the binding competent fraction can be performed, for example from enzyme activity or by binding another ligand with established enthalpy and stoichiometry. Using a calibrating ligand enables estimation of the ligand concentration, which is directly linked to the estimated enthalpy, or the protein concentration, which is linked to the estimated stoichiometry.

Control and calibration experiments are needed periodically to ensure appropriate instrument performance and optimal experimental data. The most basic control experiment is a water-water experiment, which reports on the condition of the instrument, the quality of cell cleaning and injection repeatability. When studying a new titrant molecule, control dilution experiments into the experimental buffer help to assess potential self-association or non-idealities, such as interaction with buffer components. Established standard binding experiments provide evidence of the accurate performance and calibration of the instrument. Electrical calibrations, which are performed through a dedicated resistor attached to the sample cell, are quick and easy to undertake. However, they only test the accuracy of the thermal power sensor of the ITC.

Experimental calibration with a well-established reaction is a better resource because it tests all instrumental elements: injector, stirring, heat sensor and thermostat. The calorimeter response to an electrical thermal power input may be considerably different to a chemical input for the effective time constant, as the thermal power source has a different location[47]. Reactions such as methanol or sucrose dilution, acid-base neutralization, protein-ligand interaction and oligonucleotide hybridization have all been used[26,48-50]. However, a common calibrating reaction is the chelation between ethylenediaminetetraacetic acid (EDTA) and Ca^{2+} at mildly acidic *pH*[51-53]. These chemicals are cheap and the solutions are stable for a long time. Care should still be taken as the values of K_a and ΔH^0 are quite sensitive to *pH*.

The basic protocol is applicable to many scenarios, including heterogeneous, allosteric, and polysteric systems. Although many aspects of the interacting molecules may initially be unknown — for example, if they self-associate or behave allosterically — this does not prevent determination of apparent interaction parameters. Further experimental development, guided by experimental results and additional structural or functional information helps gain a deeper insight into the interaction.

Sample loading

Samples loaded in the higher volume ITC instruments need to be degassed to avoid bubble formation during the experiment. This can be easily performed in the vacuum devices provided by manufacturers. Practical experience suggests that the small volume instruments are less dependent on degassing, so this step can be omitted. With the exception of the fully automated instruments, the ITC is loaded manually, with gas-tight syringes in a careful procedure to avoid trapping any air during loading.

Cleaning

Cleaning the instrument is key to obtaining good quality data. To reach high-sensitivity levels for heat detection, cells are not removable and are only accessible through loading tubes. Therefore, cells must be cleaned extensively by flushing to guarantee that the instrument is ready for a new experiment. Manual flushing creates turbulence inside the cells that helps to guarantee effective cleaning. After cleaning, an extensive water purge can also be conducted using the vacuum cleaning devices provided. Fully automated instruments include an automated cleaning set-up, where detergent cleaning is followed by alcohol rinsing and extensive water flushing. For strong aggregation, precipitation, or sample components that adhere to the inner cell surface, harsher cleaning may be needed, such as using a surfactant solution at room temperature or higher, or even NaOH/HCl solution in severe situations. To check the quality of the cleaning procedure, a quick water-water run should be performed. This should be a routine quality check for users, comparing the experimental and programmed d*P* level, and the peak profile and amplitude to previous runs with the same experimental settings. Best practice is to perform a water-water run at the start and end of any set of experiments.

Data collection

The ITC instrument controls all phases of a titration experiment: thermal equilibration; recording signal while periodically injecting titrant solution aliquots; and storing the data in an output file. During this operation, the instrument controls the temperature of the adiabatic jacket surrounding the reference and sample cells, continuously measures the temperature difference between the cells and modulates changes in the applied feedback power to the sample cell. The output is a file containing the feedback thermal power at each time point, plus additional data, such as temperature in the sample cell and other instrument parameters, including the working temperature, cell volume, injection volume and reactant concentrations.

Results

Representative results

The ITC thermogram, which shows the differential thermal power — the difference power as a function of time (dP *vs* t) — before baseline correction, represents the true raw data (see **Figure 2** and **Figure 4**). Defining the baseline enables peak integration; however, it can be a subjective procedure, especially when manual adjustment is possible. Where the heats are small, careful baseline selection is required. Software-based automatic baseline drawing and correction have been developed to reduce user influence on this process. Integration of each injection peak within an appropriate time interval provides the heat effect associated with that injection. This heat effect contains contributions from the intermolecular interaction under study, plus additional unspecific effects, such as mechanical mixing, buffer solution mismatch, temperature equilibration and titrant or titrand dilution.

After baseline subtraction, an idealized flat thermogram is produced, where baseline regions have zero signal (see **Figure 2** and **Figure 4**). While these data are aesthetically pleasing, there is a loss of information, such as signal drift, baseline stepping or low frequency fluctuations. As a result, in publications, it is encouraged to present the uncorrected raw data that shows the chosen baseline and the resulting peak integrals.

Using the individual heat effects per injection, derived from integrated peaks in μJ or μcal, the binding isotherm can be constructed by plotting heat values as a function of the advance of the binding reaction. Two basic isotherms can be drawn: the cumulative heat curve, where each data point is equal to the total heat measured up to that injection; or the differential, also referred to as the difference, heat curve, where each data point is equal to the individual heat associated with each injection. The cumulative signal curve is the most common representation in other binding techniques, while the differential individual heat effect representation is favored by the ITC community. Using the differential heat isotherm has some notable advantages over the cumulative heat isotherm.

The usual representation for the calorimetric isotherm, the Wiseman isotherm, was introduced in a seminal paper[35]. The titrant-normalized heat effect per injection (in J/mol or cal/mol) is plotted as a function of the molar ratio, the quotient between total titrant concentration and total titrand concentration in the sample cell: $\frac{Q_j}{v[X]_0}$ *vs* $\frac{[X]_{T,j}}{[M]_{T,j}}$ (**Figures 2**, **4** and **5**). Because individual heat values are normalized by the amount of titrant injected into the cell, the y-axis variable can be considered as an incremental quotient. Alternative representations to the Wiseman isotherm have been proposed, such as one where the heat effect is not normalized and the reaction progress is represented by the cumulative volume added from the injection syringe or the titrant concentration: Q_j *vs* v_T, or Q_j *vs* $[X]_T$ (see **Supplementary Information,** section **Is the Wiseman isotherm an appropriate representation?** and **Figure 5**)[54]. These alternative representations have the advantage of including the titrant or titrand concentrations, which can be uncertain or unknown, as fitting parameters, something that is not possible with the Wiseman isotherm.

After baseline correction and peak integration, the binding isotherm can be used to estimate the binding parameters. This is achieved by selecting an appropriate binding model and fitting to the experimental data using a NLLS regression, coupled with an efficient iterative minimization procedure, such as the Levenberg-Marquardt algorithm. The basic procedure consists of the following steps (see **Supplementary Information**, section **Flow chart for ITC data analysis**). First, the concentrations of titrant and titrand inside the cell are calculated before and after each titrant injection (see **Box 2**). Next, the binding model is defined, specifying the chemical species and equilibrium constants (see **Box 3**). Once the binding model is defined, the conservation

equations for titrant and titrand (see **Box 3**) are written. After each injection, the conservation equations are solved analytically or numerically, either as a set of nonlinear equations with two unknowns — the concentration of free titrant and free titrand — or a single nonlinear equation with a single unknown — the concentration of free titrant — using initial tentative values for the equilibrium constants. Concentration changes for each complex after each titrant injection are calculated and the incremental changes in complex concentration are determined after each injection (see **Box 3**). The theoretical value of the heat effect per injection is then calculated by using the initial tentative value of the formation enthalpies of the complexes and their concentration changes along each injection (see **Box 3**) By comparing the calculated and experimental heat values, the fitting parameters can be modified if needed. The previous steps are repeated until the desired level of convergence is attained: χ^2, the sum-of-the-squared-residuals, lower than a predefined value, or no longer able to be minimized.

The operator is only involved in binding model selection and initial estimates. All the other steps are calculated by the fitting programs. After fitting, the quality of the regression must be judged. It is good practice to check if the same parameter estimates are obtained using different initial estimates, to exclude the possibility that fitting has converged on a secondary, non-global minimum in χ^2.

Often, the titrand is a protein that has an uncertain active or binding-competent concentration. The parameter *n* accounts for this imprecision, providing the effective percentage of active or binding-competent fractions. If all concentrations are correct, the fitting procedure should provide a value, within error, of 1 for *n* when using a 1:1 model. If a different value is obtained, it indicates a possible error in the measured concentrations, providing the 1:1 binding model is correct. For example, if the estimated value for *n* is 0.7, it can be concluded that 70% of the titrand is able to interact with the titrant (**Figure 5**). Recalculating the concentrations of titrand after each injection and applying this renormalization factor gives $n = 1$. Similarly, *n* can absorb uncertainties from titrant concentration errors. It could also be concluded that $n = 0.7$ arises from there being ($1/0.7\times100=$) 142% of titrant in the syringe, in other words, the titrand concentration is underestimated by 42%. Care must be taken when judging *n* values. For example, if $n = 0.5$, it may be concluded that either only 50% of titrand is binding-competent, or that there is a 100% excess of titrant in the syringe. An equally valid interpretation is that each titrant molecule binds two titrand molecules (1:2, titrant:titrand binding model).

In more complex situations, uncertainties in the titrand and titrant might occur simultaneously. It is useful to note that obtaining $n = 1$ does not guarantee an absence of errors in the determined concentrations, because they may cancel each other. For instance, an overestimation of titrand concentration together with an underestimation of titrant concentration.

In summary, it is possible to determine the concentration of one interacting molecule if the concentration and stoichiometry of the other molecule are precisely known. The correct concentration for the uncertain reactant gives $n = 1$ in the fitting procedure.

Data analysis

NLLS fitting of the experimental binding isotherm involves comparison of the theoretical isotherm (Q_{calc}), obtained from initial binding parameters (see **Box 3**), with the experimental isotherm (Q_{exp}), These parameters are modified to minimize the least-squares difference between both curves:

$$\chi^2 = \sum_{j=1}^{m} \left(Q_{calc,j} - Q_{exp,j}\right)^2 \quad (2)$$

The procedure is repeated until convergence and χ^2 is no longer reduced based on the set threshold. Once the calculation has converged, nominal values of the estimated parameters and their fitting errors are obtained. Sometimes, the distance between the theoretical and experimental isotherms is quantified using the reduced-χ^2. This is achieved by introducing the

fitting degrees of freedom — $m - p$, the number of experimental points in the binding isotherm minus the number of estimated parameters — as a normalizing factor in the denominator.

The optimal situation for parameter estimation corresponds to one where binding affinity and enthalpy can be simultaneously and reliably estimated. This occurs when the c parameter lies between 1 and 10000, though optimally between 10 and 1000. For c values higher than 10000, the binding affinity cannot be estimated because all binding isotherms for extreme affinity (K_d < 0.1 nM) superimpose, meaning affinity differences cannot be distinguished. When this occurs, only a lower limit for K_a and a higher limit for K_d can be derived. For c values lower than 1, insufficient curvature and the absence of an inflection point in the binding isotherm result in correlation, or degeneracy, of the binding parameters, preventing proper estimation (see figures in **Box 2**).

The optimal binding model is one that is able to reproduce the experimental data with minimal complexity. In complex situations with more than one binding site, it is possible to keep adding binding sites, with the aim of the new binding model providing a better fit to the experimental data. However, this often results in convergence failure and correlation between estimated parameters. Any complexity element added to the binding model must be evaluated for its ability to improve the fit with a statistical test. Incorrect accounting for the background injection heat often leads to addition of spurious binding sites, with unrealistic binding parameters.

Although NLLS fitting is the most common tool for ITC data analysis, Bayesian analysis has also been used. Bayesian analysis has the advantage of including information about different experimental uncertainties and correlations, such as the reactant concentrations[55].

The background injection heat term

Titrant and titrand dilution heats, plus the background injection heat are important factors in data analysis. The background injection heat represents the main cause of incorrect analysis[27,56]. This contribution to the global heat effect needs to be accounted for or subtracted from the total measured heat per injection and can be estimated in different ways. The magnitude and sign can be obtained through a control experiment, by injecting the titrant into a buffered solution. However, this experiment may not faithfully reflect what happens in the actual interaction experiment. Alternative methods are often used to determine a value. For example, by calculating the average heat effect for the last few injections in a given titration. This approach only works with high affinity and when sufficient titrant has been added to reach saturation. Alternatively, a value for the background term can be included during fitting. This can be a constant value or a titrant concentration-dependent term, for example a value that is proportional to the molar ratio or the increment in free titrant concentration inside the cell. This procedure can be applied in any titration, but is particularly applicable when saturation is not reached. When the background injection heat cannot be included in the fitting routine and control experiments are not available, the fitting will be compromised (see **Figure 5**). To make the fitting curve go through the experimental points, it may be tempting to use more complex binding models that introduce additional spurious binding sites, usually with negligible affinity and extremely large binding enthalpy. However, this is not advised as it has a similar impact to adding too many binding sites in the binding model: the fitting procedure will either be affected by overparameterization and correlation/degeneracy between parameters, or some parameters will have unrealistic values.

Model evaluation and uncertainty report

When fitting a given titration with two different models, usually visual inspection, nominal estimated parameter values, and χ^2 are enough to decide which model is more appropriate. Sometimes the difference between two models is subtle. Parametric (F-test, for nested models) and non-parametric (Akaike or Bayesian information criteria) tests can be applied to select the best model. These tests are all based on the χ^2 value, number of data points (m), and number of estimated parameters (p). The aim is to judge whether an improved fit, represented by a smaller

χ^2, from adding one more parameter is due to more parameters being used. In other words, they are statistical significance tests for differences.

The estimated binding parameter values should be critically considered. A good fit does not only rely on a theoretical curve passing through the data points, but also requires reasonable binding affinities and enthalpies. For example, a binding enthalpy of ±400 kJ/mol would be suspicious.

When reporting data from an ITC ligand binding study, it is essential to assign the uncertainty and repeatability of each parameter and to describe how this estimate was obtained. Extensive repeat measurements are usually not possible in biological investigations. However, a reasonable number of experiments should be conducted to enhance the robustness of the retrieved parameters. Technical and biological replicates are recommended to assess instrument performance and preparation variability. Technical replicates consist of experiment repetitions using the same sample, while biological replicates consist of experiment repetitions with different samples for the same interaction. Typical systematic error sources that should be considered are errors in reactant concentrations, effective cell volume, poor baseline stability, heat sensor calibration, and reactant concentrations due to adsorption to the calorimeter and aggregation or misfolding along the titration[31,56-58]. An important but usually overlooked error source is the way the background heat effect, or heat of dilution, is accounted for[27,56].

ITC instruments include software to calculate the thermodynamic binding parameters with an estimate of their fitting errors. These errors only reflect the goodness of a model fit to a particular set of results. A complete error estimate for the parameters must be obtained by repeating the measurement. Uncertainties from the fit can be given as symmetric parametric errors (based on the t-Student distribution), or profile likelihood asymmetric confidence intervals (based on the F-Snedecor distribution)[59]. Although the first approach is more commonly used, for a parameter with an error <10%, for example ΔH^0 or n, both ways are equivalent. Otherwise, the most appropriate method to specify uncertainty is to use an asymmetric confidence interval. This is particularly relevant for equilibrium constants, K_a or K_d [59].

To decrease uncertainty, it may be possible to globally fit several replicates — which decreases the uncertainty by a factor of the square root of the number of replicates — or to individually fit several replicates and calculate the average parameter values and their standard deviations. Calculations for equilibrium constants (K_a and K_d) must be performed using the geometric average and the geometric standard deviation. By contrast, enthalpies and other energies require the arithmetic average and arithmetic standard deviation[59].

Data analysis can be performed in other dedicated software. For example, NITPIC is a freely available software for ITC baseline fitting and peak integration[60]. NITPIC-treated data can be output to a file that can be read and subsequently fit with other ITC software. SEDPHAT is a freely available software that can import data from NITPIC[61,62]. SEDPHAT uses NLLS to obtain the standard thermodynamic parameters and reports possible linkage parameters for simple bimolecular interactions. It can analyse multi-site and multicomponent systems with competition or cooperativity. SEDPHAT can also perform global analysis and does not use the traditional approach of a binding model with the parameter n as the stoichiometry value. Instead, it provides concentration correction factors. The factors account for errors in the reactant's concentrations or the presence of non-active forms of the protein. A significant number of binding models are offered, together with global multi-method analysis. SEDPHAT provides parameter errors in the form of confidence intervals for the chosen level of statistical significance. AFFINImeter is a versatile commercial software package for ITC, which has some simple models built-in, while allowing many complex models to be built in an intuitive manner through a graphic interface[63]. Software choice can be daunting, but a recent benchmark study compared how these programmes treated the same data, for a simple 1:1 binding[53].

In this Primer, the standard protocol for ITC has been discussed. A brief description of advanced protocols can be found in the **Supplementary Information**.

Applications

Molecular recognition, the specific interaction between two molecules through non-covalent forces, plays an important role in biological systems. Almost all biological processes involve the interaction of at least two molecules. The first area where ITC experiments can be used is to provide evidence on whether or not two molecules interact. A single experiment reporting equal, small heat effects is not sufficient to rule out any interaction, but detection of systematic, decreasing heat effects above the background is indicative of an interaction taking place, although dilution controls are always needed. Once it has been established that two molecules are able to interact, the next questions relate to the strength, interaction type, responsible functional groups and the influence of environmental variables, such as temperature, *pH* and ionic strength. Carefully designed ITC experiments can address these questions and yield the thermodynamic binding profile of an interaction. Changes in the experimental conditions or structure of the interacting molecules will be reflected in changes in this profile.

Binding studies

The simplest biological interaction is a single ligand binding site in a protein. A variety of possibilities may arise, from low to very high affinity, and highly exothermic to highly endothermic binding. This results in a range of thermodynamic binding profiles, reflecting the intermolecular forces underlying the biological interaction. Protein-DNA interaction is an example. The partially disordered methyl-CpG binding domain (MBD) of the transcriptional regulator MeCP2 is able to discriminate between unmethylated and methylated cytosine[64]. MBD and DNA interact with moderate affinity and very small positive enthalpy. However, when MBD is flanked by two disordered domains, its affinity for DNA dramatically increases by 400 times. The enthalpy of binding is more favorable — ΔH^0 changes from +4 kJ/mol to –200 kJ/mol — suggesting a different mode of interaction. It is likely that a conformational change in MBD underlies this allosteric phenomenon. One of the additional domains is able to bind another DNA molecule, making the new construction a two-binding site protein.

A protein with two binding sites is the next complexity level. There are several possibilities: identical or non-identical sites; and independent or cooperative sites, with each binding site displaying the many possibilities of a single binding site[65]. The binding model for a protein with several binding sites can be defined in terms of the overall binding constants or step-wise binding constants, which are equivalent formulations. Often, step-wise binding is referred to as the sequential binding model. However, this is misleading because the formulation does not consider sequential occupation of the binding sites in the protein following an ordered process. The relationship between the overall or step-wise constants with the intrinsic site-specific constants and the cooperativity parameters can be established for any binding model, although it may be operationally meaningless for a complex situation. It is important that ITC users are aware of the many subtleties around mathematical formalism, binding models and their implementation during data analysis, to adequately interpret the results.

ITC can provide a comprehensive biophysical characterization to describe how a protein discriminates different ligands, how a ligand induces a population shift in a protein's conformational equilibrium, or how a mutation hinders an interaction resulting in pathogenic potential. For example, the archaeal transporter GltPh, an aspartate-sodium symporter, shows a weak affinity for aspartate in the absence of sodium. In the presence of sodium, the aspartate affinity is considerably increased[66]. This is a compulsory linked binding with positive heterotropic cooperativity between aspartate and sodium and positive homotropic cooperativity between sodium atoms. The affinity of each individual ligand is low, and a 10-fold increase in sodium concentration results in 400-fold increase in aspartate binding affinity. Heterotropic interactions can be easily studied using the Wyman plot of $\log K_d$ *vs* $\log[S]$, where S is a secondary

ligand binding cooperatively with the main ligand[67]. GltPh is a transmembrane protein. To study GltPh by ITC, samples are prepared with a solubilizing detergent over its critical micelle concentration. Membrane proteins were classically extracted with surfactant micelles and reconstituted into liposomes. Recently, however, membrane proteins have been transferred to lipid nanodiscs surrounded by membrane scaffold proteins or polymers, such as diisobutylene/maleic acid copolymer. The reconstituted proteins are closer to their membrane physiological environment, and can be studied by ITC[68]. Another example is the interaction of the fifth module of the low-density lipoprotein (LDL) receptor, which is a key element for the interaction with LDL. The fifth module can interact with Ca^{2+} and Mg^{2+} ions. The protein's conformational stability is strongly influenced by *pH* and cation concentrations, a coupling that is instrumental for the regulation of cargo binding, internalization, and receptor recycling back to the plasma membrane[69,70]. A third example is the heterotropic interaction with positive cooperativity between ATP/ADP and Mg^{2+} in their interaction with α- and β-subunits of the F1-ATPase, which is coupled to the homotropic cooperativity of Mg^{2+} ions binding to ATP[71,72].

Often, homotropic cooperativity is a consequence of the quaternary structure of proteins, from identical or similar subunits. This is not a strict requirement, as single chain proteins, such as ovotransferrin and calmodulin can bind several ligands, such as iron and calcium, respectively. Additionally, all proteins have more than one ionizable group, representing binding sites for protons. The molecular basis for allosteric cooperativity is a protein conformational landscape modulated by ligand binding. There are distinguishable conformational states with different ligand affinities. Presence of the ligand stabilizes and increases the population of states that it best interacts with. The study of homotropic cooperativity by applying a complete ensemble of conformational and ligation states, known as the general allosteric model[73] may be impractical for more than two ligand binding sites. Two simplifying models were developed to address this: Monod-Wyman-Changeux[74,75] and Koshland-Némethy-Filmer[76-80]. A detailed discussion on these models, their similarities and disparities, is beyond the scope of this Primer. However, both models have been implemented in ITC for studying the cooperative interaction of oligomeric proteins with ligands.

It has been proposed that drug design and development could be guided and accelerated by adding thermodynamic profiles as diagnostic criteria to optimize drug candidates. This would consider binding affinity, selectivity and allosterism, where enthalpy is a key descriptor[13,14,16,20,81-83]. Interesting results have been reported when applying a thermodynamic guide for drug design[20,81]. A favorable binding enthalpy, with exothermic binding, is considered a desirable feature for specific protein binders with high potential for optimization and high selectivity. However, some results were obtained in a retrospective manner and others with congeneric compounds. As a result, there is controversy on the limitations and practical utility of the thermodynamic guide for drug optimization. A plethora of possible additional equilibria may be coupled to the binding interaction, meaning it may be challenging to derive the intrinsic thermodynamic binding profile for a given interaction[84]. Nevertheless, differences in the thermodynamic binding profiles of different molecules under the same experimental conditions may provide valuable insight into their modes of interaction. A single technique cannot offer a complete description of binding mechanisms, but ITC, taken together with other experimental techniques, can help to fully unravel the details of the system under study.

Partition to lipid membranes

Another interesting development is the study of surfactants, drugs, or proteins interacting with lipid membranes using formalism based on the partition constant, K_P [85-92]. Traditionally, partition constants were determined by spectroscopy, but the advent of high-sensitivity ITC instruments has enabled them to be used in this field. ITC has a clear advantage, as together with K_P, the partition binding enthalpy, ΔH_P, can be simultaneously estimated. If experiments are performed at different temperature, ΔC_P, can also be derived, which is a fundamental property in partition to

membranes. The phenomenological approach is different from ligand-binding, as partition of the solute from the aqueous solution to the membrane, which must be considered as another phase, or a pseudo-phase. In other words, the solute partitions between the two media. Appropriate data treatment leads to the observed partition coefficient, K_P^{obs}, given by the ratio of solute concentrations in each phase. The main implication is that there are no specific binding site(s) as in ligand binding, but a partition between two media. The ligand is the titrand that will be titrated with lipid from the syringe, and the isotherm will be a plot of *Q vs* total lipid concentration. When performing experiments with lipid membranes, for example large unilamellar vesicles or liposomes, a particular experimental setup consists of injecting a lipid dispersion into the binding molecule solution. This setup intends to minimize non-idealities and avoid lipid membrane saturation, which has been proven to distort the estimated binding parameters[91] (**Figure 6**).

Use of ITC to study partition to membranes has been hindered by less established data analysis procedures that are not part of the instrument software. Many users do not use ITC for this purpose and, when it is used, the data is treated as a binding event. Two data analysis worksheets for partition followed by ITC are freely available upon request[91,92].

Biotechnology and biomedicine

ITC is not capable of the high-throughput required for initial compound screening in drug discovery. However, it is good for validating screening protocols and target engagement, to provide direct evidence of hits or candidates interacting with the targets. It has been widely used by drug development companies, such as Vertex (USA), together with other biophysical characterization techniques[9,93]. In preclinical studies, ITC can be used in drug optimization and development by providing information on affinity, selectivity, ligand-induced conformational changes and partition of drugs to membranes. In the final preclinical stages, ITC may help to design optimized formulations for biotechnological or biomedical products, creating quality control tests based on affinity, enthalpy of binding, and active concentration determination.

The interaction of molecules with long linear macromolecules, for example, antibiotic binding to DNA or proteins binding to long linear charged polymers, is another binding model with biomedical and biotechnological interest. In this case, there are no well-defined individual binding sites, but a large set of overlapping binding sites of certain polymer subunit length. The binding model to be applied is the McGhee-von Hippel model[94], which is valid for long polymer chains and accounts for the intrinsic apparent negative binding cooperativity[95-97]. This model can account for cooperativity effects between neighboring bound molecules.

ITC may help to assess different macromolecular constructs — structural protein variants for chemical or physical stability, or functional protein variants obtained by protein engineering and redesign — by evaluating the affinity and specificity of the interaction with binding partners, or to assess heterogeneous enzyme catalysis[98]. Further discussion of ITC's applications in biotechnology and biomedicine can be found in elsewhere[99-101].

Novel approaches

Developments using ITC have recently been suggested. One example involves the determination of kinetic association and dissociation constants, as an important added capability to the equilibrium binding information accessible by ITC. Previous attempts to determine kinetic rates by calorimetry were mainly directed at moderately slow enzymatic reactions, to circumvent the influence of the instrumental time constant. The first successful attempts, such as kinITC, were based on a detailed description and analysis of the time evolution of the thermal power, the calorimetric raw data[102]. A later, much simpler, development was based on the equilibration time

curve (ETC), which evaluates the time required to return to baseline for the injection peaks along a given calorimetric titration[103-105]. It is a well-known phenomenon that the peak width broadens as the molar ratio approaches the equivalence point, due to slower kinetics when fewer titrant-free titrand molecules are available. After passing the equivalence point, the peak width decreases as there is less binding. Analysis of the ETC curve, together with the equilibrium dissociation constant K_d, enables estimation of k_{on} and k_{off} for the binding. Kinetic results from ITC were in agreement with results from purely kinetic techniques, such as surface plasmon resonance[105].

Another successful use of ITC to determine kinetics was recently published[106]. The d*P vs* t trace, the thermogram, was used to extract k_{on} and k_{off} for the interaction. The method and program were tested using two well-studied systems, and the obtained kinetic parameters were in very good agreement with the literature. Importantly, best practices were proposed for both experiments and data treatment, referred to as kinetically optimized ITC.

Studies of protein oligomerization induced by ligand binding is another novel use of ITC. This is a macroscopic reflection of the coupling between oligomerization and binding equilibria. It represents an important regulation mechanism of protein conformation and ligand binding if the monomer and oligomer conformation display different binding affinities for the ligand. An example of this situation is the interaction of sodium dodecyl sulphate with by β-lactoglobulin, which forms weak homodimers at neutral *pH*. ITC was instrumental for analyzing the coupled-equilibria and revealed that ligand binding promotes dimer dissociation, showing that the ligand has a lower affinity to the dimer[107,108]. Data analysis software is available on request to provide fitting tools for coupled complex equilibria, in particular, self-aggregating molecules[109].

ITC was very recently applied to monitor surface phenomena at the air-liquid interface. By injecting air into liquid inside the calorimetric cell, it was possible to follow the formation, growth and release of air bubbles and the corresponding heat/power signals[110,111]. By measuring the bubble formation period at a certain air flow rate, the surface tension of pure liquids and their mixes were measured, with good agreement to other techniques. This opens the possibility of extending the ITC methodology to determine liquid-liquid interfacial tension and monitor the adsorption of amphipathic molecules on interfaces.

Other developments relate to studies of interaction-condensation processes, for example cations and small molecules on DNA, which has special relevance to liquid-liquid phase separation, coacervates, and membraneless organelles in cells[112-114]. Further developments look at studying interactions of small and large molecules in non-aqueous solvents.

Reproducibility and data deposition

Available repositories

Few repositories contain ITC data from biological interactions, and there are currently no established standards for ITC data storage. BindingDB is an open-access database of measured binding affinities for drug-target proteins with small, drug-like molecules. BindingDB contains data from a variety of experimental techniques, including ITC, and has 41,296 entries, each containing 2,533,459 binding data for 8,811 protein targets and 1,085,985 small molecules. SCORPIO is a small open-access database currently holding data from 29 different proteins, 176 ligands and 90 unique protein-ligand complexes with both ITC and structural data. The aim of SCORPIO is to provide access to complete thermodynamic profiles for protein-ligand complexes that have had their structures resolved. There is also a NIST reference database of the thermodynamics of enzyme catalyzed reactions, available along with access to a computer package BioEqCalc that enables treatment of complex equilibria in solution. The output provides a wide range of information, such as molarities, mole fractions, and activity coefficients of reactants and solvent (H_2O), alongside relevant thermodynamic parameters — apparent

equilibrium constants K_{eq}', standard transformed Gibbs free energies $\Delta_r G'^0$ and standard transformed enthalpies of reaction $\Delta_r H'^0$ [115].

Minimum reporting standards

Binding parameters are usually strongly dependent on experimental conditions. Changes in temperature, *pH*, ionic strength, and additives affect the binding affinity and enthalpy. When reporting thermodynamic interaction data, it is crucial to provide a clear description of the experimental conditions and details of the sample preparation to ensure reproducibility. A minimal set of quality control assays, based on identity, purity, homogeneity, and integrity, must be applied to the sample for a protein (see **Supplementary Information,** section **Protein sample quality**). Elemental analysis can be applied to low molecular weight compounds to confirm their purity. In addition, a complete description of the experimental and instrumental settings must also be provided, including the raw unprocessed data together with final analyzed data.

Reproducibility issues

There is a general reproducibility issue in Science, which several publications have highlighted over a range of scientific disciplines[116,117]. Poor-quality reagents and reference materials, including proteins and peptides, is often at the heart of this problem in biological sciences (see **Supplementary Information,** section **Protein sample quality**). The limited space in publications means there is little room for a detailed description of the sample preparation procedures, the experimental protocol, and, most importantly, the potential caveats and critical steps. It is often not possible to compare experimental results because critical pieces of information are missing in publications or repositories. To provide complete and relevant information on biological experiments, several aspects need to be taken into account: samples should be subjected to a quality control test; experimental protocols should be extensively detailed, including control and calibration experiments; and a comprehensive description of the data analysis must be given.

When comparing results in different publications on a particular interaction, consideration should be given to the possible experimental variation. Differences can arise from changing the interacting molecules, for instance, protein sequence, added labels or tags; dissimilar sample preparation protocols; different experimental protocols or data analysis tools. If all aspects are the same, an additional point is whether the results are significantly different, considering the assigned uncertainties. To assess this, the results must be significantly different statistically, with confidence intervals that do not intersect, and also significantly different practically. Further clarification using the *p*-value may be meaningless if the size-effect, the difference in the discordant values, is negligible or has unimportant practical consequences. However, it is possible for a difference to be statistically significant (p-value < 0.05) by artificially increasing the size of the sample or number of replicates. As a result, common sense and the usual uncertainties for binding parameters must be taken into consideration when comparing experimental results. This is not only to judge reproducibility, but also to evaluate the effect of a protein mutation on an interaction or the impact of an activator binding on substrate binding. In practice, as a rule of thumb, affinities closer than a 5-fold factor and enthalpies closer than 2 kJ/mol (0.5 kcal/mol) may be considered similar.

Limitations and optimizations

Accessible information

ITC monitors the rapid encounter between two interacting molecules. It records the transitory thermal power effect in the first minutes after titrant addition and the successful encounter between interacting molecules. Any kinetically slow process with a large time constant will occur unnoticed, hidden within the noise and variability of the baseline. Compared to other binding techniques, which operate at a steady-state endpoint and record a signal after a long incubation time, ITC can be considered a transient effect technique. It may be possible to overlook high affinity interactions because the high affinity binding conformation is attained after a long time, more than several minutes. Only the moderate or low affinity binding conformation is detected. It is not uncommon to derive binding affinities by ITC that are lower than those determined by steady-state spectroscopic techniques[118,119]. This is due to a further step to accommodate the slow, high-affinity binding conformation that remains undetected within the baseline fluctuations.

The binding parameters determined in a single experiment are apparent thermodynamic interaction parameters, which correspond to those particular experimental conditions, not necessarily only the interaction of interest. Many additional coupled equilibria may contribute to the apparent binding parameters. In particular, one of the main additional extrinsic contributions corresponds to buffer ionization. Ionizable groups in the titrant or the titrand will also contribute as an extrinsic contribution. Even if the reactants (de)ionization is considered intrinsic, since it is inherent to the interaction, it will be *pH* dependent. This means it can vary with the environment, causing it to have non-intrinsic character. Additional coupled equilibria contributing to the observed interaction parameters mean additional experimental planning and work is necessary to remove those contributions and determine the intrinsic thermodynamic profile for the interaction. All these considerations are crucial when interpreting the binding parameters in a structural context or when reporting experimental conditions.

There is a practical window for affinity determination, which depends on the c parameter. However, there is a more stringent limitation for very high affinity ($c > 10000$), where K_a and K_d are ill-defined, but ΔH^0 and n are uncorrelated and can be reliably determined. At very low affinity ($c < 1$) the binding affinity (K_a or K_d) becomes uncorrelated from ΔH^0 and n, and its estimation is fairly robust and independent[34]. This means ΔH^0 and n remain strongly correlated at low c values. Fixing one is required to reach convergence in the iterative fitting analysis. Workarounds exist based on modified protocols, such as competition and displacement experiments, to determine extreme affinities without needing to modify the experimental conditions, or resorting to arbitrary or subjective decisions during data analysis.

A potential limitation comes from the dependence of the measured signal on the reaction enthalpy. If the binding enthalpy is close to zero, no information on the interaction can be obtained from the ITC assay. Instead, a set of small, similar sized peaks would be recorded and a meaningless flat isotherm would result. It is possible to mistakenly conclude that an interaction is not occurring when the binding enthalpy is close to zero. Fortunately, the binding enthalpies in biological interactions are usually strongly temperature-dependent due to a significant change in heat capacity. This provides a workaround for studying interactions in this scenario (see **Supplementary Information,** section **Calorimetry measures heat, but… what if enthalpy is zero?**).

When a fractional unexpected value is obtained, there are multiple interpretations of the parameter n (see **Figure 5**). This issue does not arise in other techniques because they use cumulative isotherms, where total measured signal is a function of the reaction advance, which show less sensitivity to n than difference isotherms used in ITC. When a fractional value of n is estimated, and the 1:1 stoichiometry has been confirmed by other means, the titrand or titrant concentrations can be corrected.

Equipment limitations

One of the main criticisms of ITC is that it is a time- and sample-consuming technique. However, many other biophysical techniques use comparable sample quantities — such as nuclear magnetic resonance spectroscopy and small-angle X-ray scattering — or may require significant assay development or protocol optimization over long time-scales, with considerable overall sample consumption, for example surface plasmon resonance. Other techniques — fluorescence spectroscopy, microscale thermophoresis, microfluidic diffusional sizing, biolayer interferometry — can determine binding affinities with much less sample. However, ITC is the only method that provides two layers of thermodynamic information (affinity and enthalpy) for a given biological interaction. Careful experimental design in ITC helps optimize sample consumption and current instrumentation uses less than one fifth of the volume and less than one third of the running time of earlier ITCs. Fully automated versions of these small volume ITCs with unattended operation are available, addressing some issues related to throughput.

Calibration

To produce good, reliable and accurate data, instrument calibration and user training are crucial. On delivery, all calorimeters are calibrated for basic parameters, such as heat sensing, cell and syringe delivery volume. These must be checked regularly and corrected during use if necessary. The only way to ensure accurate and comparable data is to regularly calibrate the calorimeter and use test procedures.

Progressive automation in ITC instruments has led to a reduced user intervention, removing one of the main sources of variability. Automation has also facilitated ITC's use by non-expert users. Today, many ITC users are not extensively trained in calorimetry, and it is important to develop and strengthen skills and abilities, with a culture of calibration and testing. To achieve this, the main causes of error and critical operational points must be understood, with easy-to-use, well-established calibration and testing procedures.

Electrical calibration can be used to produce very precise calibration values. Despite this, the accuracy is, in most cases, compromised due to construction constraints, such as the heater position. This causes the heat flow to follow a pattern different to a reaction in solution. Worse, systematic errors are often introduced[56]. This implies that chemical reaction should be used instead, and many publications have addressed this issue, resulting in different test reactions for ITC[26,53,120-122]. For many years, test reactions involved proteins or enzymes, but these were difficult to standardize appropriately. The currently accepted ITC calibration and test reactions are simple chemical reactions, as these chemicals can be easily obtained with very high purity and the solutions are easy to prepare in a reproducible way. Examples are the binding of Ca^{2+} and Mg^{2+} to EDTA under precisely defined experimental conditions[53]; the protonation of 2-amino-2-(hydroxymethyl)-1,3-propanediol or the reaction of Ba^{2+} with 1,4,7,10,13,26-hexaoxacyclooctadecane (18-Crown-6)[26,120,122]; or simple propanol dilution[121], although some of these reactions are strongly dependent on the experimental conditions. These test reactions can be used to periodically check the accuracy of the ITC and to train new users. Calibration and training go hand in hand to generate good practices that improve reproducibility and accuracy[27,31].

The two important take home messages are that meaningful data requires ITC instruments to be calibrated with an appropriate test reaction, and the determined thermodynamic parameters must be correctly reported and thoroughly described, with a full uncertainty evaluation.

Outlook

Instruments must be further improved to increase throughput with smaller samples quantities and reduced experimental time. Better instruments may also widen the practical window for affinity determination without needing advanced protocols and improve the specific sensitivity, the minimum amount of heat per unit of volume. This would require further technological advances for detecting or processing signals. The basic limitation for the minimum detectable signal is not the current signal noise level (around 1 nW in current instruments), but the water-to-water injection heat effect. The heat effect associated with this injection is the lowest value of the measurable heat. This is because the water-to-water heat effect contains several of the unspecific contributions to the observed heat effect in any study. Regardless of improvements to the heat detection, if the water-to-water heat effect is present, it will limit the lowest heat that can be effectively detected by the instrument. This is one of the reasons, among others, to maintain a thoroughly clean instrument.

An additional way to increase throughput would be to develop instruments that allow parallel measurements. A multichannel isothermal calorimeter was designed by Thermometrics AB, now sold by TA Instruments, that monitors up to 48 channels. Recently, conjugating miniaturization and parallel operation enthalpy micro-arrays have been developed at SYMCEL, with calScreener. They highlight the potential use for microcalorimetry in the development of antimicrobials, thermogenesis studies and cancer biology. Both approaches are non-titrating instruments, but batch ones instead. Implementing a titration capability may represent a challenge.

Another alternative approach is the flow calorimeter, where titrand and titrant solutions are continuously pumped through an elongated cell, while increasing the titrant concentration. A new development of this calorimeter type was recently reported[123]. This design could be easily automated for high-throughput testing of many titrants against a certain titrand molecule. However, the current automated step-wise titration calorimeters provide higher quality data, avoiding the complications of the flow calorimeter, such as potential conflict between residence time in the cell and the binding reaction kinetics.

ITC has become the gold standard for studying intermolecular interactions in solution. Among its many advantages, some can be highlighted. It does not require immobilization or chemical modification with chromogenic or fluorogenic labels, which might distort or hamper the interaction. ITC provides many layers of information — affinity, enthalpy and entropy, heat capacity, and linkage parameters — using a simple experimental set-up with little assay development that enables direct determination of the affinity and the enthalpy of binding without relying on the van't Hoff equation. The technique is particularly suited to studying macromolecules with several binding sites and cooperative binding phenomena. Finally, it allows a broad range of affinity determination and provides kinetic information. Membrane-associated proteins can also be studied given appropriate sample preparation, which is important as membrane proteins are principal targets in drug discovery. If needed, non-aqueous solvents can be used for inorganic or organic small-molecule and supramolecular chemistry.

The last two decades have seen hyperbolic growth in the number of experimentally determined atomic-resolution 3D-structures of macromolecules and macromolecular assemblies. Coupled with high-performance, artificial intelligence predictions of a protein's 3D-structures, notably by AlphaFold, means there is now a plethora of structural data waiting to be translated into molecular mechanisms, function, and regulation. These new discoveries will have ramifications for biotechnological and biomedical applications, aided by ITC and its capability to dissect the complete thermodynamic profile of molecular interactions. Although recent developments have led to new or improved biophysical techniques — some of them not requiring immobilization or chemical labelling, for example microfluidic diffusional sizing, dynamic light scattering, and analytical ultracentrifugation — it is expected that ITC will continue to stand out among the broad set of binding techniques for studying biomolecular interactions.

Acknowledgments

The authors acknowledge the key role of ARBRE (Association of Resources for Research in Biophysics in Europe) and COST MOBIEU Action (CA15126, Between Atom and Cell: Integrating Molecular Biophysics Approaches for Biology and Healthcare, supported by COST - European Cooperation in Science and Technology) in fostering collaborations and promoting the exchange of knowledge and experience. The authors also acknowledge M. Brandts (MicroCal/Malvern-Panalytical) and C. Quinn (CSC/TA Instruments) for clarifying some technical details of their respective instruments, as well as L. Hansen (Brigham Young University, Provo, UT, USA) for reading critically the parts of the text dealing with CSC/TA Instruments and for many fruitful discussions with M.B. on calorimeter design and function during the preparation of this Primer. Finally, the authors acknowledge pioneering technical work developing microcalorimeters and early studies showing the application of these instruments to biological systems from J. J. Christensen, R. M. Izatt, L. D. Hansen, S. J. Gill, R. L. Biltonen, E. Freire, J. F. Brandts, V. V. Plotnikov, P. L. Privalov, G. I. Makhatadze, J. M. Sturtevant, I. Wadsö, G. Waksman and R. N. Goldberg — without these key scientists the whole area of biocalorimetry would not be the established and widely used technique that it is today.

Author contributions

Introduction (M.B., O.A. and A.V.C.); Experimentation (M.B., C.M.J. and A.V.C.); Results (M.B., C.M.J. and A.V.C.); Applications (O.A., S.V. and A.V.C.); Reproducibility and data deposition (M.B., F.S., A.J.A. and A.V.C.); Limitations and optimizations (O.A., C.M.J., D.O.A. and A.V.C.); Outlook (F.S. and A.V.C.); Overview of the Primer (A.V.C.).

Competing interests

The authors declare no competing interests.

References

1. Christensen, J. J., Johnston, H. D. & Izatt, R. M. An isothermal titration calorimeter. *Rev. Sci. Instrum.* **39**, 1356–1359 (1968).

2. Freire, E., Mayorga, O. L. & Straume, M. Isothermal titration calorimetry. *Anal. Chem.* **62**, 950A–959A (1990).

3. Spolar, R. S., Ha, J. H. & Record, M. T. Jr. Hydrophobic effect in protein folding and other noncovalent processes involving proteins. *Proc. Natl. Acad. Sci. USA* **86**, 8382–8385 (1989).

4. Ortiz-Salmerón, E., Yassin, Z., Clemente-Jimenez, M. J., Las Heras-Vazquez, F. J., Rodriguez-Vico, F., Barón, C. & García-Fuentes, L. Thermodynamic analysis of the binding of glutathione to glutathione S-transferase over a range of temperatures. *Eur. J. Biochem.* **268**, 4307–4314 (2001).

5. Jelesarov, I. & Bosshard, H. R. Isothermal titration calorimetry and differential scanning calorimetry as complementary tools to investigate the energetics of biomolecular recognition. *J. Mol. Recognit.* **12**, 3–18 (1999).

6. Perozzo, R., Folkers, G. & Scapozza L. Thermodynamics of protein-ligand interactions: history, presence, and future aspects. *J. Recept. Signal Transduct. Res.* **24**, 1–52 (2004).

7. Claveria-Gimeno, R., Vega, S., Abian, O. & Velazquez-Campoy, A. A look at ligand binding thermodynamics in drug discovery. *Expert Opin. Drug Discov.* **12**, 363–377 (2017).

8. Johnson, C. M. Isothermal titration calorimetry. *Methods Mol. Biol.* **2263**, 135–159 (2021).

9. Holdgate, G. A. Making cool drugs hot: isothermal titration calorimetry as a tool to study binding energetics. *Biotechniques* **31**, 164–166 (2001).

10. Geschwindner, S., Ulander, J. & Johansson, P. Ligand binding thermodynamics in drug discovery: still a hot tip? *J. Med. Chem.* **58**, 6321-6335 (2015).

11. Klebe, G. Broad-scale analysis of thermodynamic signatures in medicinal chemistry: are enthalpy-favored binders the better development option? *Drug Discov. Today.* **24**, 943–948 (2019).

12. Franco, R., Bai, G., Prosinecki, V., Abrunhosa, F., Ferreira, G. C. & Bastos, M. Porphyrin-substrate binding to murine ferrochelatase: effect on the thermal stability of the enzyme. *Biochem. J.* **386**, 599–605 (2005).

13. Velazquez-Campoy, A., Todd, M. J. & Freire, E. HIV-1 protease inhibitors: enthalpic versus entropic optimization of the binding affinity. *Biochemistry* **39**, 2201-2207 (2000).

14. Velazquez-Campoy, A., Kiso, Y. & Freire, E. The binding energetics of first- and second-generation HIV-1 protease inhibitors: implications for drug design. *Arch. Biochem. Biophys.* **390**, 169–75 (2001).

15. Todd, M. J., Luque, I., Velazquez-Campoy, A. & Freire, E. Thermodynamic basis of resistance to HIV-1 protease inhibition: calorimetric analysis of the V82F/I84V active site resistant mutant. *Biochemistry* **39**, 11876–11883 (2000).

16. Vega, S., Kang, L. W., Velazquez-Campoy, A., Kiso, Y., Amzel, L. M. & Freire, E. A structural and thermodynamic escape mechanism from a drug resistant mutation of the HIV-1 protease. *Proteins* 55, 594–602 (2004).

17. Chaires, J. B. Calorimetry and thermodynamics in drug design. *Annu. Rev. Biophys.* **37**, 135–151 (2008).

18. Privalov, P. L., Dragan, A. I., Crane-Robinson, C., Breslauer, K. J., Remeta, D. P. & Minetti, C. A. What drives proteins into the major or minor grooves of DNA? *J. Mol. Biol.* **365**, 1-9 (2007).

19. Freire, E. A thermodynamic approach to the affinity optimization of drug candidates. *Chem. Biol. Drug Design* **74**, 468–472 (2009).

20. Ladbury, J. E., Klebe, G. & Freire, E. Adding calorimetric data to decision making in lead discovery: a hot tip. *Nat. Rev. Drug Discov.* **9**, 23–27 (2010).

21. Kawasaki, Y. & Freire, E. Finding a better path to drug selectivity. *Drug Discov. Today* **16**, 985–990 (2011).

22. Klebe, G. Applying thermodynamic profiling in lead finding and optimization. *Nat. Rev. Drug Discov.* **14**, 95–110 (2015).

23. Tarcsay, A. & Keseru, G. M. Is there a link between selectivity and binding thermodynamics profiles? *Drug Discov. Today* **20**, 86–94 (2015).

24. Freire, E. The binding thermodynamics of drug candidates. In *Thermodynamics and Kinetics of Drug Binding*, Keserü, G. M. & Swinney, D. C., Wiley-VCH Verlag GmbH & Co (2015).

25. Tellinghuisen, J. Calibration in isothermal titration calorimetry: heat and cell volume from heat of dilution of NaCl(aq). *Anal. Biochem.* **360**, 47–55 (2007).

26. Demarse, N. A., Quinn, C. F., Eggett, D. L., Russell, D. J. & Hansen, L. D. Calibration of nanowatt isothermal titration calorimeters with overflow reaction vessels. *Anal. Biochem.* **417**, 247–255 (2011).

27. Hansen, L. D. & Quinn, C. Obtaining precise and accurate results by ITC. *Eur. Biophys. J.* **48**, 825–835 (2019).

28. Bastos, M. & Velazquez-Campoy, A. Isothermal titration calorimetry (ITC): a standard operating procedure (SOP). *Eur. Biophys. J.* **50**, 363–371 (2021).

29. Tellinghuisen, J. Optimizing experimental parameters in isothermal titration calorimetry. *J. Phys. Chem. B.* **109**, 20027-20035 (2005).

30. Tellinghuisen J. Designing isothermal titration calorimetry experiments for the study of 1:1 binding: problems with the "standard protocol". *Anal. Biochem.* **424**, 211–220 (2012).

31. Kantonen, S. A., Henriksen, N. M. & Gilson, M. K. Evaluation and minimization of uncertainty in ITC binding measurements: heat error, concentration error, saturation, and stoichiometry. *Biochim. Biophys. Acta Gen. Subj.* **1861**, 485–498 (2017).

32. Velazquez-Campoy, A. Geometric features of the Wiseman isotherm in isothermal titration calorimetry. *J. Therm. Anal. Calorim.* **122**, 1477–1483 (2015).

33. Turnbull, W. B. & Daranas, A. H. On the value of c: can low affinity systems be studied by isothermal titration calorimetry? *J. Am. Chem. Soc.* **125**, 14859-14866 (2003).

34. Tellinghuisen J. Isothermal titration calorimetry at very low c. *Anal. Biochem.* **373**, 395–397 (2008).

35. Wiseman, T., Williston, S., Brandts, J. F. & Lin, L.-N. Rapid measurement of binding constants and heats of binding using a new titration calorimeter. *Anal. Biochem.* **179**, 131–137 (1989).

36. Christensen, J. J., Hansen, L. D. & Izatt, R. M. Handbook of Proton Ionizations Heats. Wiley-Interscience, Hoboken, NJ, USA (1976).

37. Goldberg, R. N., Kishore, N. & Lennen, R. M. Thermodynamic quantities for the ionization reactions of buffers. *J. Phys. Chem. Ref. Data* **31**, 231–370 (2002).

38. Hinz, H. J., Shiao, D. D. F. & Sturtevant, J. M. Calorimetric investigation of inhibitor binding to rabbit muscle aldolase. *Biochemistry* **10**, 1347–1352 (1971).

39. Eftink, M. & Biltonen, R. Thermodynamics of interacting biological systems. In *Biological Calorimetry*, pp. 343–412, Beezer, A. E. (ed.), Academic Press, London (1981).

40. Armstrong, K. M. & Baker, B. M. A comprehensive calorimetric investigation of an entropically driven T cell receptor-peptide/major histocompatibility complex interaction. *Biophys J.* **93**, 597–609 (2007).

41. Xie, D., Gulnik, S., Collins, L., Gustchina, E., Suvorov, L. & Erickson, J. W. Dissection of the pH dependence of inhibitor binding energetics for an aspartic protease: direct measurement of the protonation states of the catalytic aspartic acid residues. *Biochemistry* **36**, 16166-16172 (1997).

42. Baker, B. M. & Murphy, K. P. Evaluation of linked protonation effects in protein binding using isothermal titration calorimetry. *Biophys. J.* **71**, 2049–2055 (1996).

43. Velazquez-Campoy, A., Luque, I., Todd, M. J., Milutinovich. M., Kiso, Y. & Freire, E. Thermodynamic dissection of the binding energetics of KNI-272, a potent HIV-1 protease inhibitor. *Protein Sci.* **9**, 1801–1809 (2000).

44. Grimsley, G. R. & Pace, C. N. Spectrophotometric determination of protein concentration. *Curr. Protoc. Protein Sci.* **33**, 3.1.1 (2003).

45. Gill, S. C & von Hippel, P. H. Calculation of protein extinction coefficients from amino acid sequence data. *Anal. Biochem.* **182**, 319–326 (1989).

46. Pace, C. N., Vajdos, F., Fee, L., Grimsley, G., & Gray, T. How to measure and predict the molar absorption coefficient of a protein. *Protein Sci.* **11**, 2411–2423 (1995).

47. Velazquez-Campoy, A., Lopez-Mayorga, O. & Cabrerizo-Vilchez, M. A. Determination of the rigorous transfer function of an isothermal titration microcalorimeter with Peltier compensation. *J. Therm. Anal. Calorim.* **57**, 343–359 (1999).

48. Wädso, I. Needs for standards in isothermal microcalorimetry. *Thermochim. Acta.* **347**, 73–77 (2000).

49. Wädso, I. Standards in titration microcalorimetry. *Netsu Sokutei* **28**, 63–67 (2001).

50. Baranauskiene, L., Petrikaite, V., Matuliene, J. & Matulis, D. Titration calorimetry standards and the precision of isothermal titration calorimetry data. *Int. J. Mol. Sci.* **10**, 2752–2762 (2009).

51. Griko, Y. V. Energetics of Ca(2+)-EDTA interactions: calorimetric study. *Biophys. Chem.* **79**, 117–127 (1999).

52. Rafols, C., Bosch, E., Barbas, R. & Prohens, R. The Ca2+–EDTA chelation as standard reaction to validate isothermal titration calorimeter measurements (ITC). *Talanta* **154**, 354–359 (2016).

53. Velazquez-Campoy, A., Claro, B., Abian, O., Höring, J., Bourlon, L., Claveria-Gimeno, R., Ennifar, E., England, P., Chaires, J. B., Wu, D., Piszczek, G., Brautigam, C., Tso, S. C., Zhao, H., Schuck, P., Keller, S. & Bastos, M. A multi-laboratory benchmark study of isothermal titration calorimetry (ITC) using Ca2+ and Mg2+binding to EDTA. *Eur. Biophys. J.* **50**, 429–451 (2021).

54. Hansen, L. D., Transtrum, M. K. & Quinn, C. F. Titration calorimetry from concept to application. Springer Briefs in Molecular Science, Spring International Publishing (2018).

55. Nguyen, T. H., Rustenburg, A. S., Krimmer, S. G., Zhang, H., Clark, J. D., Novick, P. A., Branson, K., Pande, V. S., Chodera, J. D. & Minh, D. D. L. Bayesian analysis of isothermal titration calorimetry for binding thermodynamics. *PLoS One* **13**, e0203224 (2018).

56. Tellinghuisen, J. & Chodera, J. D. Systematic errors in isothermal titration calorimetry: concentrations and baselines. *Anal. Biochem.* **414**, 297-299 (2011).

57. Wadsö, I. & Wadsö, L. Systematic errors in isothermal micro- and nanocalorimetry. *J. Thermal Anal. Calorim.* **82**, 553–558 (2005).

58. Tellinghuisen, J. Volume errors in isothermal titration calorimetry. *Anal. Biochem.* **333**, 405–406 (2004).

59. Paketurytė, V., Petrauskas, V., Zubrienė, A., Abian, O., Bastos, M., Chen, W. Y., Moreno, M. J., Krainer, G., Linkuvienė, V., Sedivy, A., Velazquez-Campoy, A., Williams, M. A. & Matulis, D. Uncertainty in protein-ligand binding constants: asymmetric confidence intervals versus standard errors. *Eur. Biophys. J.* **50**, 661–670 (2021).

60. Keller, S., Vargas, C., Zhao, H., Piszczek, G., Brautigam, C. A. & Schuck, P. High-precision isothermal titration calorimetry with automated peak-shape analysis. *Anal. Chem.* **84**, 5066-5073 (2012).

61. Zhao, H., Piszczek, G. & Schuck, P. SEDPHAT – a platform for global ITC analysis and global multi-method analysis of molecular interactions. *Methods* **76**, 137–148 (2015).

62. Brautigam, C. A., Zhao, H., Vargas, C., Keller, S. & Schuck, P. Integration and global analysis of isothermal titration calorimetry data for studying macromolecular interactions. *Nat. Protoc.* **11**, 882-894 (2016).

63. Piñeiro, A., Muñoz, E., Sabin, J., Costas, M., Bastos, M., Velazquez-Campoy, A., Garrido, P. F., Dumas, P., Ennifar, E., Garcia-Rio, L., Rial, J., Perez. D., Fraga, P., Rodriguez, A. & Cotelo, C. AFFINImeter: A software to analyze molecular recognition processes from experimental data. *Anal. Biochem.* **577**, 117–134 (2019).

64. Claveria-Gimeno, R., Lanuza, P. M., Morales-Chueca, I., Jorge-Torres, O. C., Vega, S., Abian, O., Esteller, M. & Velazquez-Campoy, A. The intervening domain from MeCP2 enhances the DNA affinity of the methyl binding domain and provides an independent DNA interaction site. *Sci. Rep.* **7**, 41635 (2017).

65. Freire, E., Schön, A. & Velazquez-Campoy A. Isothermal titration calorimetry: general formalism using binding polynomials. *Methods Enzymol.* **455**, 127–55 (2009).

66. Boudker, O. & Oh, S. Isothermal titration calorimetry of ion-coupled membrane transporters. *Methods* **76**, 171–182 (2015).

67. Vega, S., Abian, O. & Velazquez-Campoy, A. Handling complexity in biological interactions. J. *Therm. Anal. Calorim.* **138**, 3229–3248 (2019).

68. Rajarathnam, K. & Rösgen, J. Isothermal titration calorimetry of membrane proteins - progress and challenges. *Biochim. Biophys. Acta.* **1838**, 69–77 (2014).

69. Arias-Moreno, X., Velazquez-Campoy, A., Rodriguez, J. C., Pocovi, M. & Sancho, J. Mechanism of low density lipoprotein (LDL) release in the endosome: implications of the stability and Ca2+ affinity of the fifth binding module of the LDL receptor. *J. Biol. Chem.* **283**, 22670-22679 (2008).

70. Arias-Moreno, X., Cuesta-Lopez, S., Millet, O., Sancho, J. & Velazquez-Campoy, A. Thermodynamics of protein-cation interaction: Ca(+2) and Mg(+2) binding to the fifth binding module of the LDL receptor. *Proteins* **78**, 950–961 (2010).

71. Pulido, N. O., Salcedo, G., Perez-Hernandez, G., Jose-Nuñez, C., Velazquez-Campoy, A. & Garcia-Hernandez, E. Energetic effects of magnesium in the recognition of adenosine nucleotides by the F(1)-ATPase beta subunit. *Biochemistry* 49, 5258–5268 (2010).

72. Salcedo, G., Cano-Sanchez, P., de Gomez-Puyou, M. T., Velazquez-Campoy, A. & Garcia-Hernandez, E. Isolated noncatalytic and catalytic subunits of F1-ATPase exhibit similar, albeit not identical, energetic strategies for recognizing adenosine nucleotides. *Biochim. Biophys. Acta.* **1837**, 44–50 (2014).

73. Wyman, J. & Gill, S. J. Binding and linkage: functional chemistry of biological macromolecules. Mill Valley: University Science Books (1990).

74. Monod, J., Wyman, J. & Changeux, J.-P. On the nature of allosteric transitions – a plausible model. *J. Mol. Biol.* **12**, 88–118 (1965).

75. Felix, J., Weinhäupl, K., Chipot, C., Dehez, F., Hessel, A., Gauto, D. F., Morlot, C., Abian, O., Gutsche, I., Velazquez-Campoy, A., Schanda, P. & Fraga, H. Mechanism of the allosteric activation of the ClpP protease machinery by substrates and active-site inhibitors. *Sci. Adv.* **5**, eaaw3818 (2019).

76. Koshland, D. E. Jr, Némethy, G. & Filmer, D. Comparison of experimental binding data and theoretical models in proteins containing subunits. *Biochemistry* **5**, 365–385 (1966).

77. Claveria-Gimeno, R., Velazquez-Campoy, A. & Pey, A. L. Thermodynamics of cooperative binding of FAD to human NQO1: Implications to understanding cofactor-dependent function and stability of the flavoproteome. *Arch. Biochem. Biophys.* **636**, 17–27 (2017).

78. Taneva, S. G., Bañuelos, S., Falces, J., Arregi, I., Muga, A., Konarev, P. V., Svergun, D. I., Velazquez-Campoy, A. & Urbaneja, M. A. A mechanism for histone chaperoning activity of nucleoplasmin: thermodynamic and structural models. *J. Mol. Biol.* **393**, 448–463 (2009).

79. Ruiz-Ramos, A., Velazquez-Campoy, A., Grande-Garcia, A., Moreno-Morcillo, M. & Ramon-Maiques, S. Structure and functional characterization of human aspartate transcarbamoylase, the target of the anti-tumoral drug PALA. *Structure* **24**, 1081–1094 (2016).

80. Freiburger, L. A., Baettig, O. M., Sprules, T., Berghuis, A. M., Auclair, K. & Mittermaier, A. K. Competing allosteric mechanisms modulate substrate binding in a dimeric enzyme. *Nat. Struct. Mol. Biol.* **18**, 288–294 (2011).

81. Velazquez-Campoy, A. & Freire, E. Incorporating target heterogeneity in drug design. *J. Cell Biochem.* **Suppl 37**, 82–88 (2001).

82. Velazquez-Campoy, A., Muzammil, S., Ohtaka, H., Schön, A., Vega, S. & Freire, E. Structural and thermodynamic basis of resistance to HIV-1 protease inhibition: implications for inhibitor design. *Curr Drug Targets Infect Disord.* **3**, 311–328 (2003).

83. Ohtaka, H., Muzammil, S., Schön, A., Velazquez-Campoy, A., Vega, S. & Freire, E. Thermodynamic rules for the design of high affinity HIV-1 protease inhibitors with adaptability to mutations and high selectivity towards unwanted targets. *Int. J. Biochem. Cell Biol.* **36**, 1787–1799 (2004).

84. Krimmer, S. G. & Klebe G. Thermodynamics of protein-ligand interactions as a reference for computational analysis: how to assess accuracy, reliability and relevance of experimental data. *J. Comput. Aided Mol. Des.* **29**, 867–883 (2015).

85. Heerklotz, H. & Seelig, J. Titration calorimetry of surfactant–membrane partitioning and membrane solubilization. *Biochim. Biophys. Acta* **1508**, 69–85 (2000).

86. Heerklotz, H. Membrane stress and permeabilization induced by asymmetric incorporation of compounds. *Biophys. J.* **81**, 184–195 (2001).

87. Keller, S., Heerklotz, H. & Blume, A. Monitoring lipid membrane translocation of sodium dodecyl sulfate by isothermal titration calorimetry. *J. Am. Chem. Soc.* **128**, 1279-1286 (2006).

88. Keller, S., Heerklotz, H., Jahnke, N. & Blume, A. Thermodynamics of lipid membrane solubilization by sodium dodecyl sulfate, *Biophys. J.* **90**, 4509–4521 (2006).

89. Heerklotz, H. & Seelig, J. Leakage and lysis of lipid membranes induced by the lipopeptide surfactin. *Eur. Biophys. J. Biophys. Lett.* **36**, 305–314 (2007).

90. Heerklotz, H., Tsamaloukas, A. D. & Keller, S. Monitoring detergent-mediated solubilization and reconstitution of lipid membranes by isothermal titration calorimetry. *Nat. Protoc.* **4**, 686–697 (2009).

91. Moreno, M. J., Bastos, M. & Velazquez-Campoy, A. Partition of amphiphilic molecules to lipid bilayers by isothermal titration calorimetry. *Anal. Biochem.* **399**, 44–47 (2010).

92. Vargas, C., Klingler, J. & Keller, S. Membrane partitioning and translocation studied by isothermal titration calorimetry. *Methods Mol. Biol*. **1033**, 253–271 (2013).

93. Connelly, P. An account in calorimetric research: from fundamentals to pharmaceuticals. In *Biocalorimetry. Foundations and contemporary approaches* (Ed. Bastos, M.), CRC Press, Taylor & Francis Group, New York (2016).

94. McGhee, J. D. & von Hippel, P. H. Theoretical aspects of DNA-protein interactions: co-operative and non-co-operative binding of large ligands to a one-dimensional homogeneous lattice. *J. Mol. Biol.* **86**, 469–489 (1974).

95. Velazquez-Campoy, A. Ligand binding to one-dimensional lattice-like macromolecules: analysis of the McGhee-von Hippel theory implemented in isothermal titration calorimetry. *Anal. Biochem.* **348**, 94–104 (2006).

96. Kasimova, M. R., Velazquez-Campoy, A. & Nielsen, H. M. On the temperature dependence of complex formation between chitosan and proteins. *Biomacromolecules* **12**, 2534–2543 (2011).

97. Water, J. J., Schack, M. M., Velazquez-Campoy, A., Maltesen, M. J., van de Weert, M. & Jorgensen, L. Complex coacervates of hyaluronic acid and lysozyme: effect on protein structure and physical stability. *Eur. J. Pharm. Biopharm.* **88**, 325–331 (2014).

98. Westh, P. & Borsh, K. Calorimetric assays for heterogeneous enzyme catalysis calorimetric assays for heterogeneous enzyme catalysis: hydrolysis of cellulose and biomass. In *Biocalorimetry. Foundations and contemporary approaches* (Ed. Bastos, M.), CRC Press, Taylor & Francis Group, New York (2016).

99. Krell, T. Microcalorimetry: a response to challenges in modern biotechnology. *Microb. Biotechnol.* **1**, 126–136 (2008).

100. Schön, A. & Velazquez-Campoy, A. Calorimetry. In *Methods for Structural Analysis of Protein Pharmaceuticals* (Eds. Crommelin, D. J. A., Jiskoot, W.), in Biotechnology: Pharmaceutical Aspects Series, AAPS Press, Virginia, USA, vol. 3, pp. 573–589 (2005).

101. Baranauskiene, L., Kuo, T. C., Chen, W. Y. & Matulis, D. Isothermal titration calorimetry for characterization of recombinant proteins. *Curr. Opin. Biotechnol.* **55**, 9–15 (2019).

102. Zihlmann, P., Silbermann, M., Sharpe, T., Jiang, X., Mühlethaler, T., Jakob, R. P., Rabbani, S., Sager, C. P., Frei, P., Pang, L., Maier, T. & Ernst, B. KinITC-One method supports both thermodynamic and kinetic SARs as exemplified on FimH antagonists. *Chemistry* **24**, 13049–13057 (2018).

103. Egawa, T., Tsuneshige, A., Suematsu, M. & Yonetani T. Method for determination of association and dissociation rate constants of reversible bimolecular reactions by isothermal titration calorimeters. *Anal. Chem.* **79**, 2972 (2007).

104. Burnouf, D., Ennifar, E., Guedich, S., Puffer, B., Hoffmann, G., Bec, G., Disdier, F., Baltzinger, M. & Dumas, P. kinITC: a new method for obtaining joint thermodynamic and kinetic data by isothermal titration calorimetry. *J. Am. Chem. Soc.* **134**, 559–565 (2012).

105. Dumas, P., Ennifar, E., Da Veiga, C., Bec, G., Palau, W., Di Primo, C., Piñeiro, A., Sabin, J., Muñoz, E. & Rial, J. Extending ITC to kinetics with kinITC. *Methods Enzymol.* **567**, 157–180 (2016).

106. Tso, S.-C., Jowitt, T. A. & Brautigam, C. A. The feasibility of determining kinetic constants from isothermal titration calorimetry data. *Biophys. J.* **121**, 2474–2484 (2022).

107. Bello, M., Portillo-Tellez, M. del C. & Garcia-Hernandez, E. Energetics of ligand recognition and self-association of bovine β-lactoglobulin: differences between variants A and B. *Biochemistry* **50**, 151–161 (2011).

108. Gutierrez-Magdaleno, G., Bello, M., Portillo-Tellez, M. C., Rodriguez-Romero, A. & Garcia-Hernandez, E. Ligand binding and self-association cooperativity of β-lactoglobulin. *J. Mol. Recognit.* **26**, 67-75 (2013).

109. Saeed, I. Q. & Buurma, N. J. Analysis of isothermal titration calorimetry data for complex interactions using I2CITC. *Methods Mol. Biol.* **1964**, 169–183 (2019).

110. Garrido, P. F., Bastos, M., Velazquez-Campoy, A., Dumas, P. & Piñeiro, A. Fluid interface calorimetry. *J. Colloid Interface Sci.* **596**, 119–129 (2021).

111. Garrido, P. F., Bastos, M., Velazquez-Campoy, A., Amigo, A., Dumas, P. & Piñeiro, A. Unsupervised bubble calorimetry analysis: Surface tension from isothermal titration calorimetry. *J. Colloid Interface Sci.* **606**, 1823–1832 (2022).

112. Utsuno, K. & Uludağ, H. Thermodynamics of polyethylenimine-DNA binding and DNA condensation. *Biophys. J.* **99**, 201–207 (2010).

113. Kim, W., Yamasaki, Y., Jang, W.-D. & and Kataoka K. Thermodynamics of DNA condensation induced by poly(ethylene glycol)-block-polylysine through polyion complex micelle formation. *Biomacromolecules* **11**, 1180–1186 (2010).

114. Basak Kayitmazer, A. Thermodynamics of complex coacervation. *Adv. Colloid Interface Sci.* **239**, 169–177 (2017).

115. Akers, D. L., & Goldberg, R. N. BioEqCalc: A package for performing equilibrium calculations on biochemical reactions. *Mathematica J.* **8**, 86-113 (2001).

116. Freedman, L. P., Cockburn, I. M. & Simcoe, T. S. The economics of reproducibility in preclinical research. *PLoS Biol.* **13**, e1002165 (2015).

117. Baker, M. 1,500 scientists lift the lid on reproducibility. *Nature* **533**, 452–454 (2016).

118. Cremades, N., Velazquez-Campoy, A., Freire, E. & Sancho, J. The flavodoxin from Helicobacter pylori: structural determinants of thermostability and FMN cofactor binding. *Biochemistry* **47**, 627-639 (2008).

119. Bollen, Y. J., Westphal, A. H., Lindhoud, S., van Berkel, W. J. & van Mierlo. C. P. Distant residues mediate picomolar binding affinity of a protein cofactor. *Nat. Commun.* **3**, 1010 (2012).

120. Briggner, L.-E. & Wadsö, I. Test and calibration processes for microcalorimeters, with special reference to heat conduction instruments used with aqueous systems. *J. Biochem. Biophys. Meth.* **22**, 101–118 (1991).

121. Adão, R., Bai, G., Loh, W. & Bastos, M. Chemical calibration of isothermal titration calorimeters: An evaluation of the dilution of propan-1-ol into water as a test reaction using different calorimeters, concentrations, and temperatures. *J. Chem. Thermodyn.* **52**, 57–63 (2012).

122. Sgarlata, C., Zito, V. & Arena, G. Conditions for calibration of an isothermal titration calorimeter using chemical reactions. *Anal. Bioanal. Chem.* **405**, 1085–1094 (2013).

123. Vaz, I. C. M., Torres, M. C., Silva, F. M. T., Carpinteiro, F. S. & Santos, L. M. N. B. F. µFlowCal – High-resolution differential flow microcalorimeter for the measurement of heats of mixing. *Chemistry – Methods* **2**, e202100099 (2022).

124. Di Trani, J. M., Moitessier, N. & Mittermaier, A. K. Measuring rapid time-scale reaction kinetics using isothermal titration calorimetry. *Anal. Chem.* **89**, 7022–7030 (2017).

125. Glöckner, S. & Klebe, G. Simultaneous determination of thermodynamic and kinetic data by isothermal titration calorimetry. *Biochim. Biophys. Acta Gen. Subj.* **1865**, 129772 (2021).

126. Broecker, J., Vargas, C. & Keller, S. Revisiting the optimal c value for isothermal titration calorimetry. *Anal. Biochem.* **418**, 307–309 (2011).

127. Sigurskjold, B. W. Exact analysis of competition ligand binding by displacement isothermal titration calorimetry. *Anal. Biochem.* **277**, 260-266 (2000).

128. Wyman, J. Linked functions and reciprocal effects in hemoglobin – A second look. *Adv. Protein Chem.* **19**, 223–286 (1964).

129. Wyman, J. The binding potential, a neglected linkage concept. *J. Mol. Biol.* **1965**, 631–44 (1965).

130. Schellman, J. A. Macromolecular binding. *Biopolymers* **14**, 999–1018 (1975).

Highlighted references

11. Ladbury, J. E., Klebe, G. & Freire, E. Adding calorimetric data to decision making in lead discovery: a hot tip. *Nat. Rev. Drug Discov.* **9**, 23–27 (2010).
This paper reviews how thermodynamic information (enthalpy and affinity) provided by ITC can help in lead discovery and optimization.

18. Hansen, L. D. & Quinn, C. Obtaining precise and accurate results by ITC. *Eur. Biophys. J.* **48**, 825–835 (2019).
This paper discusses precision and accuracy levels in binding parameters achievably ITC, emphasizing the problem associated with the background injection heat effect.

25. Tellinghuisen J. Isothermal titration calorimetry at very low c. *Anal. Biochem.* **373**, 395–397 (2008).
This paper shows that affinity estimates in ITC may be reliable at low c values.

26. Wiseman, T., Williston, S., Brandts, J. F. & Lin, L.-N. Rapid measurement of binding constants and heats of binding using a new titration calorimeter. *Anal. Biochem.* **179**, 131–137 (1989).
This paper presents the first commercially available ITC instrument, together with the most widely employed data representation, the Wiseman isotherm.

28. Goldberg, R. N., Kishore, N. & Lennen, R. M. Thermodynamic quantities for the ionization reactions of buffers. *J. Phys. Chem. Ref. Data* **31**, 231–370 (2002).
This paper contains thermodynamic parameters for the aqueous ionization of the most common biological buffers, being of paramount importance for ITC experimental design and data analysis.

60. Wyman, J. & Gill, S. J. Binding and linkage: functional chemistry of biological macromolecules. Mill Valley: University Science Books (1990).
This book presents the foundations of physical chemistry of macromolecules and represents a basic reading for any researcher in structural and functional aspects of biological macromolecules.

81. Moreno, M. J., Bastos, M. & Velazquez-Campoy, A. Partition of amphiphilic molecules to lipid bilayers by isothermal titration calorimetry. *Anal. Biochem.* **399**, 44–47 (2010).

This paper reports the adequate methodology to estimate intrinsic parameters for membrane interaction with ionic/nonionic solutes, providing a spreadsheet for data analysis.

94. Burnouf, D., Ennifar, E., Guedich, S., Puffer, B., Hoffmann, G., Bec, G., Disdier, F., Baltzinger, M. & Dumas, P. kinITC: a new method for obtaining joint thermodynamic and kinetic data by isothermal titration calorimetry. *J. Am. Chem. Soc.* **134**, 559–565 (2012).
This paper presents the most current methodology to extract thermodynamic and kinetic interaction parameters from a single ITC experiment.

117. Sigurskjold, B. W. Exact analysis of competition ligand binding by displacement isothermal titration calorimetry. *Anal. Biochem.* **277**, 260-266 (2000).
This paper presents the exact application of ternary equilibrium for ITC displacement experiments, which allow extending the practical range for affinity determination (K_d's below nM and above mM).

Boxes

Box 1: **Binding affinity scale**

The binding affinity in biological interactions is quantified using the association constant, K_a or dissociation constant, K_d. The latter is more common in biochemistry because it has a practical interpretation as the free ligand concentration required to reach 50% saturation in a macromolecule with a single ligand binding site. Equilibrium constants should be dimensionless, achieved by applying a normalization factor equal to the standard concentration (1 M) to any equilibrium concentration. However, assigning units to them is a common practice.

The adjectives low, moderate and high that are applied to the binding affinity may have different implications in different fields. For example, in natural product interaction a K_d = 1 μM for an inhibitor-target may be considered a high binding affinity, whereas the same K_d value for an antibody-antigen interaction may be considered a low binding affinity.

In general, low binding affinity is considered when K_d > 10 μM, moderate binding affinity when 0.01 μM < K_d < 10 μM, and high binding affinity when K_d < 0.01 μM.

As a real experimental example, the following figure shows the interaction of porcine pancreatic ribonuclease A (RNase A) with three isomers: 2'-, 3'-, and 5'-cytidine monophosphate (15 mM potassium acetate buffer, *pH* 5.5, 25 °C). The location of the phosphate group causes a considerable change in binding affinity: K_d = 0.34 μM for 2'CMP, K_d = 3.8 μM for 3'CMP, and K_d = 240 μM for 5'CMP. Unlike in the titrations of 2'CMP and 3'CMP, no inflection point can be observed for 5'CMP.

Box 2: **Selecting the concentrations of titrand and titrant**

The concentration of titrand, $[M]_0$, must comply with two constraints. First, to produce a sigmoidal binding isotherm with a well-defined inflection point, $[M]_0$ must fulfil the following inequality (for a 1:1 stoichiometry):

$$1 < c = \frac{[M]_0}{K_d} < 10000$$

Many users further limit the *c* value to between 10 and 1000 [126]. In the following figure, titrations (**a**, thermograms; **b**, binding isotherms) with identical experimental settings have been simulated with different binding affinities: K_d = 20 μM (orange), K_d = 0.2 μM (violet), and K_d = 20 nM (green). Because $[M]_0$ = 20 μM, the c-values were: 1, 100, and 10000, respectively. If c < 1, there is no inflection point in the binding isotherm[32]. The inflection point has interesting properties: the value of the titrant-normalized heat effect is equal to ½ ΔH^0; and the slope of the binding isotherm is equal to $-¼\ \Delta H^0\ c^{1/2}$. In addition, the intercept of the binding isotherm with the y-axis is equal to $(c/(c+1))\ \Delta H^0$ [32].

The previous requirement means that the concentration of titrand must fulfil these two inequalities:

$$K_d < [M]_0 < 10000 \times K_d$$

or more stringently:

$$10 \times K_d < [M]_0 < 1000 \times K_d$$

Second, the total heat effect along the titration, which corresponds to the sum of all individual heat effects per injection, must be higher than a minimum value. If all the titrand is converted into complex, this can be written as:

$$Q_T = [M]_0 V_0 \Delta H^0 > Q_{min}$$

where V_0 is the cell volume, implying that:

$$[M]_0 > \frac{Q_{min}}{V_0 \Delta H^0}$$

The value of Q_{min} will depend on the instrument, but Q_{min} = 40 μJ is an appropriate reference value. If, for a certain interaction, K_d is 1 μM and ΔH^0 is 20 kJ/mol, then $[M]_0$ must lie between 10 μM and 10 mM. The values for $[M]_0$ obtained from these calculations may be reasonable, but they may also be impractical. For example, to reach a good *c* value, a too low concentration of titrand might be required if the binding affinity is too high, precluding measurement of a detectable amount of heat. On the contrary, the titrand concentration might be too high if the binding affinity is too low. Therefore, there will be experimental situations that can be improved using these indications, but, very often, the user must deal with very low or very high affinity.

Considering an overfilled cell and a quasi-instantaneous injection, the total concentrations of *X* and *M* inside the cell after injection j are given by:

$$[X]_{T,j} = [X]_0 \left(1 - \left(1 - \frac{v}{V_0}\right)^j\right) \quad [M]_{T,j} = [M]_0 \left(1 - \frac{v}{V_0}\right)^j$$

where $[X]_0$ is the titrant concentration in the syringe, and *v* is the injection volume. Other injection/mixing models provide equivalent relationships[127]. The molar ratio $[X]_T/[M]_T$ in the cell after injection j is given by:

$$\frac{[X]_{T,j}}{[M]_{T,j}} = \frac{[X]_0}{[M]_0} \frac{1 - \left(1 - \frac{v}{V_0}\right)^j}{\left(1 - \frac{v}{V_0}\right)^j}$$

$[X]_0$ must be selected so that the final molar ratio (after *m* injections) is at least 2. Eventually, both concentrations must be selected considering experimental requirements and practical limitations. In case the stoichiometry is not 1:1, a factor *n* (number of titrant binding sites in the titrand) multiplying $[M]_0$ must be included in the previous equations.

Box 3: **The binding equations**

The binding model is defined by specifying complexes that can be formed along the titration process. The partition function or binding polynomial, Z, represents the binding equilibrium and it is constructed with the relative statistical weights of all possible bound states [128-130]:

$$Z = \sum_{i=0}^{N} \frac{[MX_i]}{[M]} = \sum_{i=0}^{N} \beta_i [X]^i$$

where MX_i represents the complex formed by i molecules of titrant X bound to a titrand molecule M, and β_i is the overall association constant for such complex. There are N+1 binding macrostates, free titrand molecule plus N complexes, but there are many more microstates, although possible symmetries may further reduce their number. The absolute weight or population of the macrostate MX_i is given by:

$$\chi_{MX_i} = \frac{\beta_i [X]^i}{Z}$$

where Z acts as a normalization factor. The meaning, interpretation, and relation between overall, step-wise, and site-specific association constant can be found elsewhere[73]. For simplicity, only the overall constants will be considered. Z contains all information about the binding landscape: the average number of bound titrant molecules per molecule of titrand, n_{XB}, and the average excess enthalpy, $\langle \Delta H \rangle$:

$$n_{XB} = \frac{\partial \ln Z}{\partial \ln [X]} = \frac{[X]_B}{[M]_T} \quad \langle \Delta H \rangle = RT^2 \frac{\partial \ln Z}{\partial T}$$

This expression leads to coupled chemical equilibrium with mass conservation:

$$[M]_T = [M] + [M]_B = \sum_{i=0}^{N} [MX_i] = \sum_{i=0}^{N} \beta_i [M][X]^i$$

$$[X]_T = [X] + [X]_B = [X] + n_{XB}[M]_T = [X] + \sum_{i=0}^{N} i[MX_i] = [X] + \sum_{i=0}^{N} i\beta_i [M][X]^i$$

which, when introducing the binding polynomial, can be written as:

$$[M]_T = [M]Z$$

$$[X]_T = [X] + [M]_T \frac{\partial \ln Z}{\partial \ln [X]}$$

These equations must be solved for each pair of concentrations ($[X]_{T,j}$,$[M]_{T,j}$) after each titrant injection j , assuming β_i values, providing the unknown $[X]_j$, or the pair of unknowns $[X]_j$ and $[M]_j$, the concentrations of free titrant and titrand after injection j. These equations are usually solved numerically. For 1:1 stoichiometry, this is a quadratic equation in $[X]$. The concentration of each complex MX_i after injection j can be calculated in two ways as follows:

$$[MX_i]_j = [M]_{T,j} \frac{\beta_i [X]_j^i}{\sum_{i=0}^{N} \beta_i [X]_j^i} = \beta_i [M]_j [X]_j^i$$

These equations are the same for any binding technique. However, many other techniques use an approximation of $[X]$ by $[X]_T$, where no ligand depletion occurs due to binding. The correct hyperbolic equation in terms of $[X]$ is incorrectly applied. The error is small if binding affinity is low, but considerable for moderate and high affinity. The heat effect associated with each titrant injection j, q_j, is given by:

$$q_j = V_0 \left([P]_{T,j} \langle \Delta H \rangle_j - [P]_{T,j-1} \langle \Delta H \rangle_{j-1} \left(1 - \frac{v}{V_0} \right) \right) = V_0 \sum_{i=0}^{N} \Delta H_i^0 \left([MX_i]_j - [MX_i]_{j-1} \left(1 - \frac{v}{V_0} \right) \right)$$

where ΔH^0_i is the enthalpy change for the formation of complex MX_i, and the dilution factor $1–v/V_0$ accounts for the solution volume expelled from the cell after each titrant injection. Finally, the normalized heat effect per injection is:

$$Q_j = \frac{q_j}{v[X]_0} = \frac{V_0}{v[X]_0} \sum_{i=0}^{N} \Delta H_i^0 \left([MX_i]_j - [MX_i]_{j-1} \left(1 - \frac{v}{V_0} \right) \right) + Q_d$$

where a final term Q_d accounts for all unspecific contributions to the heat effect making up the background injection heat. Although Q_d reflects many different phenomena, it is usually named dilution heat. As the stoichiometry (N) is already implicitly considered in the binding model, it is convenient to introduce another parameter, n, accounting for a renormalization factor for the titrand concentration:

$$[M]_{T,j} = n[M]_0 \left(1 - \frac{v}{V_0}\right)^j$$

Tables

Table 1. Advantages and disadvantages of ITC as a binding technique

Advantages	Disadvantages
Heat is a universal feature of any biomolecular process. ITC can be used to study virtually any interaction in a label-free manner with no requirement for modifying interacting molecules, for example with spectroscopic tags or labels.	Heat is a universal feature of all processes, which means events unrelated to the interaction under study can also contribute to the signal, making it harder to measure and deconvolute the heat signal of interest.
Impure samples, such as crude extract or partially purified material, can be studied. Samples of high turbidity or with unwanted optical properties, such as high absorbance or auto-fluorescence, can still be used.	It is a time- and sample-consuming technique, with a relatively low throughput.
It is a technique performed in solution, with no need for immobilization of any interacting molecules. This avoids the effects of immobilization, which may cause unwanted conformational changes, distorted binding site accessibility, unspecific interactions with matrices and surfaces, modulation of entropic effects and matrix embedding.	It is a technique sometimes considered intricate, not because of the experimental set-up which is rather simple, but because of the data analysis.
It is a non-destructive technique.	Solubility of reactants can be a limiting factor because the concentration of the titrant solution in the syringe can be from hundreds of μM up to mM levels.
It requires very little assay development and has an easy experimental set-up due to its label free format.	Only accurate knowledge of the protein concentration, and the concentration of its competent fraction, allows a full retrieval of the correct thermodynamic values associated with the interaction being studied, and an interpretation of the stoichiometry value *n*.
It is the only technique able to provide the complete thermodynamic profile for the interaction between two given molecules.	The preparation of the ligand in exactly the same solution conditions as the protein can be tricky, since the protein is usually obtained in solution under certain buffer conditions. Any buffer mismatch between solutions may result in large unspecific heat effects, masking the contribution of the interaction to the heat.
Recent developments have shown that kinetic parameters (kinetic association and dissociation constants) can be determined from a calorimetric data[103-106,124,125].	

Figure legends

Figure 1. Simplified scheme of an ITC instrument. a. Current instruments have either cylindrical (left), or coin-shape cells (right). The cells (S, sample; R, reference) are enclosed inside an adiabatic jacket isolating them from the surroundings and maintaining a constant temperature. A step motor inside the syringe holder controls the plunger of an air-tight syringe that injects the titrant solution into the sample cell. Stirring ensures fast homogenization after each titrant addition. At any time, the difference in temperature between the cells is converted into voltage signal by a Seebeck effect through the thermopile (TP) and later transformed into thermal power signal. **b**. As the reactant in the syringe is added to the reaction vessel (yellow squares), it binds to the reactant in the cell (red circle with binding pocket), and the excess remains in solution in the cell.

Figure 2. Thermogram and binding isotherm. a. Typical thermogram for the interaction of EDTA with Ca^{+2} in 10 mM MES buffer, *pH* 5.60, at 25 °C in a MicroCal/Malvern-Panalytical VP-ITC. A series of 28 injections of a 1.6 mM Ca^{+2} solution (titrant, *X*) into a 0.1 mM EDTA solution (titrand, *M*), while stirring at 459 rpm, was programmed. The injection volume, *v*, was 10 µL (except the first 2-µL injection), and the cell volume, V_0, was 1.4534 mL. The raw data show baseline fluctuations and irregularities that are removed when subtracting the baseline (see inset with the final processed thermogram). **b.** Close-up view of the fifth peak showing the downward deflection from an exothermic binding. **c.** Binding isotherm constructed by integrating all peaks in the thermogram and plotting them as a function of the advance of the reaction, in this case, the ratio between titrant and titrand concentrations in the cell. The continuous line is the fitting curve to a 1:1 binding. The estimated binding parameters were: K_a = 9.98 × 10^5 M^{-1} [9.64 × 10^5, 1.3 × 10^6], ΔH^0 = −17.8 kJ/mol [−17.9, −17.7], n = 0.954 [0.953, 0.956], where the brackets report the confidence interval at 95% statistical significance. The inset shows the evolution of the total concentration of EDTA (red), total concentration of Ca^{+2} (black), concentration of free EDTA (green), concentration of free Ca^{+2} (orange), and the concentration of EDTA-Ca^{+2} complex (violet).

Figure 3. Determination of the heat capacity change and number of protons exchanged upon binding. Upper plots: Titrations, thermograms and binding isotherms, corresponding to a particular interaction at *pH* 7 and different temperatures: 15 °C (orange), 25 °C(violet), and 35 °C (green). The slope in the ΔH^0_{obs} *vs* temperature plot provides the binding heat capacity, ΔC_P, which is −1.2 kJ K^{-1} mol^{-1}. Lower plots: Titrations, thermograms and binding isotherms, corresponding to the same interaction at *pH* 7 using different buffers: phosphate (orange), MOPS (violet), and TRIS (green). All buffer molecules have similar pK_a's, but different ionization enthalpy: 3.6 kJ/mol (phosphate), 21.1 kJ/mol (MOPS), and 47.5 kJ/mol (TRIS). Plotting ΔH^0_{obs} *vs* $\Delta H^0_{B,ion}$ provides the number of protons exchanged between the complex and bulk solution upon binding (Δn_{H+}, from the slope), and the buffer-independent binding enthalpy (ΔH^0, intercept with y-axis), which are 0.7 and −10.8 kJ/mol, respectively. The binding affinity for this interaction for the experiment at 25 °C is: ΔG^0 = −32.5 kJ/mol, K_a = 5 × 10^5 M^{-1}, and K_d = 2 µM. The binding affinity is slightly dependent on temperature, but should not change with different buffers if they have similar pK_a's. The binding profile for this interaction at *pH* 7 and 25 °C is: ΔG^0 = −32.5 kJ/mol, ΔH^0 = −10.8 kJ/mol, $-T\Delta S^0$ = −21.7 kJ/mol, and ΔC_P = −1.2 kJ K^{-1} mol^{-1}. In this case, because both contributions, enthalpic and entropic, are negative, both contribute favorably to the binding.

Figure 4. Experimental output in current calorimeter software. Thermogram and binding isotherm corresponding Mg^{+2}/EDTA in 10 mM HEPES, 100 mM NaCl, *pH* 7.4, at 25 °C, measured in low cell volume calorimeters, in: **a.** Origin 7.0 – ITC Module, **b.** PEAQ-ITC software, and **c.** NanoAnalyze. Upper plots show the thermogram, and lower plots show the binding isotherm. Exothermic and endothermic peaks are depicted in different orientation depending on the calorimeter software. The first injection was considered for calculating the reactant concentrations in the cell, but not for the fitting analysis (note that the PEAQ-ITC software excluded it in the binding isotherm plot). Arbitrary plotting conventions may result in depiction of exothermic or endothermic heat effects as downward or upward deflections.

Figure 5. Representations of ITC data. a. The binding isotherm corresponding to the titration of EDTA with Ca^{+2} plotted in the Wiseman representation. **b.** The binding isotherm in an alternative representation of non-normalized heat effect per injection as a function of cumulative titrant added volume. **c.** Concentration renormalization of the binding isotherm. After NLLS fitting, the binding isotherm corresponding to a certain titration (green) provides the following parameters: $K_a = 1.38 \times 10^6$ M^{-1}, $\Delta H^0 = 42.1$ kJ/mol, and $n = 0.68$. When the titrand concentration is recalculated to 68% (orange), the NLLS fitting provides the following parameters: $K_a = 1.38 \times 10^6$ M^{-1}, $\Delta H^0 = 42.1$ kJ/mol, and $n = 0.98$, suggesting unaltered estimated binding parameters. When the titrant concentration is recalculated to 147% (violet), NLLS fitting provides the following parameters: $K_a = 0.98 \times 10^6$ M^{-1}, $\Delta H^0 = 29.4$ kJ/mol, and $n = 0.98$, indicating considerably lower affinity and enthalpy. **d.** Effect of injection background heat on estimated binding parameters. The orange circles correspond to the binding isotherm for a certain titration, with NLLS-estimated parameters: $K_a = 3.00 \times 10^6$ M^{-1}, $\Delta H^0 = -21.0$ kJ/mol, and $n = 1.00$. The inset shows the corresponding thermogram. The fitting routine included an adjustable parameter accounting for the background heat effect. If the fitting routine did not account for the injection background heat effect, a reasonable fit is obtained (violet), which might be considered good if the experimental data had higher noise level. The NLLS-estimated parameters are: $K_a = 0.99 \times 10^6$ M^{-1}, $\Delta H^0 = -32.4$ kJ/mol, and $n = 1.21$, namely, 3-fold lower binding affinity and 50% more enthalpy, with a 20% higher apparent stoichiometry.

Figure 6. Interaction of lipid membranes with a peptide. Thermodynamic parameters for partition of the antimicrobial peptide LFampin265-284 to a DMPC:DMPG 3:1 large unilamellar vesicles (LUVs) at 35 °C. A 40 μM peptide solution in 10 mM HEPES buffer, *pH* 7.4 was placed in the calorimetric cell and titrated with a 35 mM DMPC:DMPG 3:1 dispersion of LUVs. Fitting used a partition model with a correction for electrostatics, assuming that the peptide only partitions to the outer layer[80]. The data is represented by black circles and the fitting line by the black line. The NLLS fitting provided the thermodynamic parameters: intrinsic partition constant (corrected for electrostatics) $K_P^0 = 1.4 \times 10^3$ M^{-1} and the partition enthalpy change $\Delta H^0 = -32.9$ kJ/mol. The effective charge was also fit and the value obtained was +1.38 (peptide nominal charge is +5). The obtained fitted dilution heat, Q_d, was 0.27 kJ/mol. The insert represents the titration curve, with the raw data already corrected for the baseline. The first injection was considered for calculating the reactant concentrations in the cell, but not for the fitting analysis. Peaks 14 and 15 showed an anomalous heat effect and were not considered in the fitting analysis.

Glossary terms

Binding isotherm – calorimetric processed data, plotting the heats from peak integration as a function of the reaction progress

Desolvation – release of some, or all, of the surface-associated solvent molecules to the bulk solution.

Enthalpy – sum of the internal energy and the product of pressure and volume. It is equal to the heat transferred during a process at constant pressure and zero non-expansion work in a closed system. In a biological interaction, it reflects the net energetic balance due to noncovalent bond rupture (with solvent) and formation (between binding partners).

Entropy – contribution to the Gibbs energy that amounts to the dissipated energy that cannot be used to generate work. It is associated with order/disorder and the configurational arrangements for energy distribution over an ensemble of states. In a biological interaction, it reflects the changes in degrees of freedom along intermolecular interactions, for example, desolvation, ion/solute exchange, conformational and vibrational changes.

Gibbs energy – maximum amount of non-expansion work that can be extracted from a process in a closed system. It is a quantitative measure of the spontaneity of a chemical reaction. In a biological interaction, it reflects the binding affinity or strength of a given intermolecular interaction, the stability of the complex.

Heat capacity – amount of heat to be provided to a system to increase its temperature a certain quantity. Thermal inertia to change temperature or capability to store thermal energy in a system.

Proton ionization – (also known as deprotonation) removal or transfer of a proton from an acid form in an acid-base reaction. Ionization of buffer molecules have an associated ionization enthalpy or proton dissociation enthalpy.

Isobaric – any process performed under constant pressure.

Isothermal – any process performed under constant temperature.

Microcalorimetry – experimental technique that uses calorimeters able to detect very small amounts of heat, at μJ level.

Reverse titration – study of the same reaction exchanging the position of the reactants between cell and syringe.

Thermogram – calorimetric raw data plotting thermal power as a function of time.

Titration – step-wise addition of a reactant to another reactant. Etymologically, quantitative chemical analysis to determine the concentration (titre) of a solution using another reagent solution of known concentration.

Supplementary Information

Isothermal Titration Calorimetry

Margarida Bastos[1†], Olga Abian[2,3,4†], Christopher M. Johnson[5], Frederico Ferreira-da-Silva[6], Sonia Vega[2], Ana Jimenez-Alesanco[2], David Ortega-Alarcon[2], Adrian Velazquez-Campoy[2,3,4*]

[1] CIQUP, Institute of Molecular Sciences (IMS), Department of Chemistry and Biochemistry, Faculty of Sciences, University of Porto, Porto, Portugal

[2] Institute of Biocomputation and Physics of Complex Systems (BIFI), and Department of Biochemistry and Molecular and Cell Biology, University of Zaragoza, Zaragoza, Spain

[3] Aragon Institute for Health Research (IIS Aragon), Zaragoza, Spain

[4] Biomedical Research Networking Center in Hepatic and Digestive Diseases (CIBERehd), Madrid, Spain

[5] MRC Laboratory of Molecular Biology, Cambridge, UK

[6] i3S - Instituto de Investigação e Inovação em Saúde, and IBMC - Instituto de Biologia Molecular e Celular, Universidade do Porto, Porto, Portugal

Emails: Margarida Bastos, mbastos@fc.up.pt, ORCID 0000-0001-7464-3568

Olga Abian, oabifra@unizar.es, ORCID 0000-0001-5664-1729

Christopher M. Johnson, cmj@mrc-lmb.cam.ac.uk, ORCID XXX

Frederico Silva, ffsilva@ibmc.up.pt, ORCID 0000-0002-8890-4228

Sonia Vega, svega@bifi.es, ORCID 0000-0002-1232-6310

Ana Jimenez-Alesanco, ajimenez@bifi.es, ORCID 0000-0003-4726-7821

David Ortega-Alarcon, dortega@bifi.es, ORCID 0000-0003-1885-4365

Adrian Velazquez-Campoy, adrianvc@unizar.es, ORCID 0000-0001-5702-4538

* Corresponding author

† Equal contribution

Technical details of present instruments on the market

All high-sensitivity ITC instruments have a dual (or twin) cell design, *i.e.,* they have two virtually identical cells (typically 0.2–1.5 mL), the sample cell (where the solution of one of the reactants is placed) and the reference cell (containing only buffer, or water). The other reactant solution is placed in the syringe (typically 40–300 μL, although CSC/TA Instruments calorimeters allow larger syringes) from which small aliquots will be delivered to the sample cell during the titration experiment. In the case of MicroCal/Malvern-Panalytical ITC instruments (VP-ITC, ITC200 and PEAQ ITC), the syringe also acts as stirrer, by rotating at the chosen speed and having at the end of the needle a flattened or twisted paddle for improved mixing. Stirring is similar in the CSC/TA Instruments Nano ITC-LV and Nano ITC-SV, but in the Affinity ITC solute delivery and stirring are independent, a stirrer shaft with a paddle attached at the end provides the mixing, whereas the titrant solution is dispensed through a small diameter stainless steel tube that runs parallel to the stirrer, ending just above the paddle. As with the MicroCal/Malvern-Panalytical instruments, there are different paddle designs employed by TA, with claimed improvements in mixing efficiency. In the MicroCal/Malvern-Panalytical models, the cells are coin-shaped, whereas in the TA Instruments ITCs the cells are cylindrical.

A simplified scheme of an ITC instrument is shown in Figure 1 of the Primer. The temperature difference between the cells (sample and reference) is continuously monitored through a semiconductor Peltier thermopile sandwiched between them. This element consists of a large number of semiconductor junctions (thermally in parallel and electrically in series) oriented between the cells that respond to differences in temperature by creating an electromotive force (voltage, ΔV)) that is proportional to the temperature gradient (*i.e*., magnitude and polarity/sign) across the thermopile sides (Seebeck effect, $\Delta V = S \Delta T$, where S is the global Seebeck coefficient of the thermopile), which is the reciprocal effect with respect to the Peltier effect: generation of temperature gradient proportional to an electric current. The heat generated within the sample cell, as a result of a titrant addition and the formation of complex with the titrand, alters the temperature of the sample cell with respect to the reference cell, while the heat is dissipated passively by conduction and convection. The instrument automatically employs the time-dependent voltage from the Peltier element as an input, applying a certain gain, to the feedback loop that provides the modulated compensation thermal power to the sample cell with the aim of minimizing the temperature difference between both cells. This means they operate on the 'dynamic power compensation principle', *i.e*., any temperature difference is promptly cancelled by the feedback system, that either increases or decreases the power applied to the sample cell, as compared to the constant heat delivered to the reference cell (reference power). By selecting zero feedback gain the instrument will operate under a purely dissipative regime with no active power compensation. Thus, heat compensation calorimeters belong to the wider family of heat conduction calorimeters.

The heat generated within the sample cell, as a result of a titrant addition and the formation of complex with the titrand, alters the temperature of the sample cell with respect to the reference cell, while the heat is dissipated passively by conduction and convection. The instrument automatically employs the time-dependent voltage from the Peltier element as an input, applying a certain gain, to the feedback loop that provides the modulated compensation thermal power to the sample cell with the aim of minimizing the temperature difference between both cells. By selecting zero feedback gain the instrument will operate under a purely dissipative regime with no active power compensation. Thus, heat compensation calorimeters belong to the wider family of heat conduction calorimeters.

Besides the feedback system that maintains the two cells at similar temperature, another feedback system will continuously monitor the temperature difference between the reference cell and an internal thermal jacket, in order to maintain a constant temperature on the cells' surroundings (i.e., isothermal conditions). The cells are thus enclosed in an 'adiabatic' shield maintaining a constant temperature (we acknowledge Lee Hansen for providing us this figure).

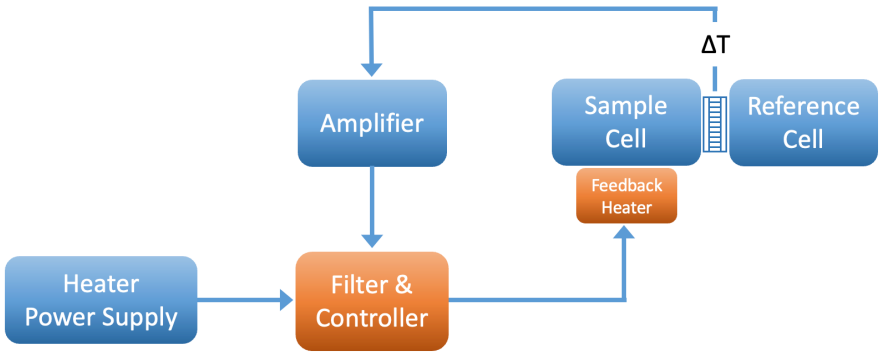

The MicroCal/Malvern-Panalytical ITCs can be used with zero feedback, heat conduction mode. The zero feedback, heat conduction mode is not available in the CSC/TA ITCs, but is the standard mode for the TA Instruments' TAM series calorimeters.

To control the system at a constant temperature, there must also be a source of cooling power. In the MicroCal/Malvern-Panalytical calorimeters this is done with a passive connection to a component controlled at a constant temperature below the temperature of the reference and reaction cells. The CSC/TA Instruments calorimeters also have a connection to an element that is colder than the reference and reaction cells, but the temperature of the cold element is actively controlled.

Heat compensation calorimeters (based on the dynamic power compensation principle) allow the user to set the baseline reference power level depending on whether the reaction is expected to be exothermic or endothermic. In the case of MicroCal/Malvern-Panalytical instruments, this constant power supplied to the reference cell defaults to (40 μW), and can be changed by the user to values between 0-140 μW. In the case of CSC/TA Instruments the user has the choice between seven explicit values referred to as 'low', 'medium', and 'high' (165 μW) which can be combined (i.e., 'low+medium', 'low+high', 'medium+high', 'low+medium+high'). This reference power on the sample cell triggers the feedback actuator on the sample cell and defines the position of the baseline.

A note on units is appropriate here - the International System of Units (SI) promotes the use of the joule (J) as unit for heat. However, traditionally calorimetrists have been using the calorie (1 calorie = 4.184 J). Presently we can see ITC results reported in both units. MicroCal/Malvern-Panalytical Origin software still provides the results in calories (in J only for graphic visualisation), but the new PEAQ-ITC software already provides all results in joules. The CSC/TA Instruments provides all results in Joules (raw data and fitted parameters).

Timeline of ITC instruments development

The first titration calorimeter, which used continuous rather than incremental titrant addition and the temperature change principle for heat measurement in specially designed Dewar flasks, was built at Brigham Young University in 1962[1] and an improved version in 1973[2]. Later improvements were commercialized by Tronac which later became CSC (Calorimetry Science Corporation, USA), which is now part of TA Instruments. TA Instruments discontinued this calorimeter when they bought CSC in 2007. Gill *et al*. designed and built the first high-sensitivity differential, heat-compensation ITC without air in the sample cell (overflow type) having a combined titration and stirring assembly[3], and 3 years later a similar instrument, with a much smaller sample volume, 200 μL[4]. In 1989 Wiseman *et al*. built a new ITC using similar principles, but using a larger sample volume (1.4 mL) and being simpler to operate[5] and other comparable instruments were developed almost simultaneously and afterwards[6-8]. In 1997 Plotnikov *et al*. built the VP-ITC[9], later commercialized by MicroCal, who is now part of Malvern-Panalytical. Presently, both companies have small volume instruments – MicroCal/Malvern-Panalytical produces the PEAQ ITC with 200 μL cell (substituting the iTC200 model), whereas TA Instruments offers two possibilities for Affinity ITC and Nano ITC – with low volume (190 μL) and standard volume (≈1 mL) cells. Although the sensitivity of the low volume models is increased, the sensitivity per volume (or specific sensitivity, the key factor) is similar. Miniaturization has made possible the use of very little sample (a few tens of nanomoles, *i.e.,* less than 1 mg of a medium size protein) in the sample cell in each assay, lowering the requirements of sample consumption, and indirectly reducing the experimentation time and cost for operation.

Sensitivity of current ITC instruments

Biological interactions are mediated by multiple weak, non-covalent interactions, resulting in very small values of the overall energetics (for example, the enthalpy of formation of a covalent bond such as C–H is –413 kJ/mol, whereas the enthalpy of formation of a non-covalent bond such as N–H···:O is –8 kJ/mol. Considering that not all weak interactions established in a macromolecule-ligand complex are contributing favourably to the binding and the competitive role of water molecules surrounding the interacting molecules, it is obvious that the observed overall binding enthalpies for biological molecules (involving many individual intermolecular interactions) are quite low: very often $|\Delta H| < 100$ kJ/mol (less than a single covalent bond).

In addition, working with biological molecules has an inherent limitation in the available concentrations (because of samples are costly and difficult to obtain, as well as labile and degradation-prone). Therefore, for monitoring and measuring the binding energetics between biological molecules it was necessary to develop very sensitive instruments. The first calorimeter able to tackle biological interactions were built in the 1960's. In current instruments the thermal power sensitivity is equivalent to detecting the transient effect of the thermal power emitted by 60 W incandescent light bulb crossing a surface of 1 cm^2 at a distance of 100 m (~0.05 μJ/s or μW).

Data collection and output files in present instruments

In the case of MicroCal/Malvern-Panalytical instruments, the output file is a text file (.itc) that can be read by any text editor and can be processed with either the MicroCal Origin ITC module, the

new PEAQ-ITC software or available data processing programs such as NITPIC[10-11], in order to properly define the baseline and proceed with the time integration of each injection peak, together with the calculation of titrant and titrand concentrations inside the cell. Afterwards, the binding isotherm can be analysed applying the NLLS fitting tool in MicroCal Origin ITC, or it can be analysed with other software packages (*e.g.,* GraphPad, Mathematica…), as well as using other data treatment programs available as e.g., SEDFAT[10-12], referred to in the main text. One of the advantages of Origin is that is quite versatile to define new fitting routines for advanced binding models and provides a convenient graphic interface to control the fitting process.

In the CSC/TA Instruments calorimeters the output file is a binary file (.nitc or .jet) that is read with the software NanoAnalyze, but the data can also be exported from NanoAnalyze and saved during collection or exported after the experiment with NanoAnalyze as a plain.csv text file. Further, as mentioned below, other available software can open and analyse these TA binary files, *e.g.,* NITPIC and AFFINImeter[13-14]. NanoAnalyze is employed to define the baseline and integrate the injection peaks, together with the calculation of titrant and titrand concentrations inside the cell. After that, the binding isotherm can be analysed by applying NLLS fitting tools with the available models or, if a suitable model is not available, models can be added by the user.

Dealing with signal overshooting

Most users of MicroCal/Malvern-Panalytical calorimeters employ high gain, since it produces the fastest experiments, as the curve is dynamically corrected to return to the baseline at the fastest rate. However, for low enthalpy reactions a zero-feedback gain may be more appropriate. High gain may result in signal overshooting, which may be avoided by selecting medium or no feedback gain (Figure S1). CSC/TA instruments use a digital filter as well as an amplifier on the temperature difference signal, and the filter time constant, which is user accessible, serves the same purpose as the amplifier gain.

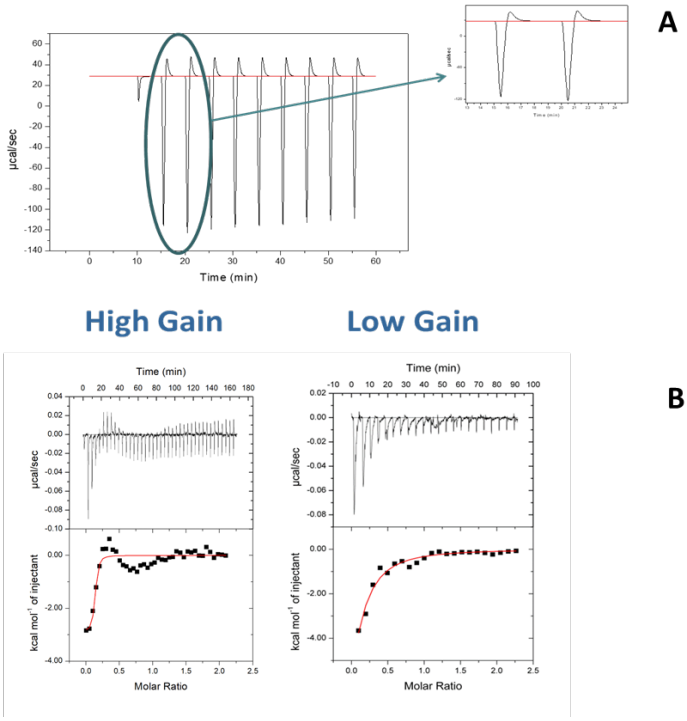

Figure S1. High/low gain and overshooting. A. The effect of overshooting can be observed when the reference power is too low. First, the thermal power signal shows a large downward deflection, followed by a steep upward recovery crossing the baseline, before returning to the baseline. The effect is clearer in the close-up view of two peaks on the right. B. The overshooting is clear when high feedback gain is used, as well as the unexpected multiphasic binding isotherm and the very bad fitting to a 1:1 interaction (left). When low feedback gain is used (with larger time spacing between injections), the signal returns to baseline between injections and a nicer binding isotherm curve is obtained after integration with a better fitting.

Advanced protocols

The basic protocol can be applied to any situation in which a titrant molecule interacts with a titrand molecule, irrespective of the additional potential features of the interaction such as polysteric interaction, *i.e.,* oligomerization equilibrium coupled to binding equilibrium, or allosteric interaction, *i.e.,* conformational equilibrium coupled to binding equilibrium, or binding equilibrium coupled to binding equilibrium). However, there are some special types of interaction requiring modifications to the basic protocol.

Homo-oligomerization of a macromolecule. This process can be easily studied by ITC, provided that the oligomerization equilibrium is dominated by the monomer and the complete oligomer, *i.e.,* intermediate states of differing molecularity are negligible. Intermediate states can of course be included but add complexity to the model and increase the chances for overparameterization and correlation between estimated parameters which will compromise fitting convergence during data analysis. The basic set-up for studying homo-oligomerization is simply to place a concentrated solution of macromolecule in the syringe (where oligomer conformation will be favoured), and perform injections into buffered solution. Each injection will trigger the dilution and concomitant dissociation of the oligomers into monomers, which will have an associated heat. From the dilution isotherm, the dissociation constant and the dissociation enthalpy may be estimated, which are the inverse and opposite of the association constant and enthalpy, respectively. This protocol has been successfully applied to homo-oligomeric proteins[15-18].

Interaction of a macromolecule with several identical ligand molecules. Many proteins are capable of such interaction, corresponding to homotropic cooperativity. Some of them exhibit a quaternary structure with several subunits responsible for the ligand binding and for the intersubunit interactions responsible for the cooperativity features, but there are also single-chain, monomeric proteins capable of such interaction. In fact, it can be stated that all proteins are capable of homotropic interaction, since almost all of them may interact with protons at well-defined ionisable sites; the proton being a special type of ligand. A macromolecule with two binding sites is the minimum homotropic model, in which the sites can be classified as identical or different, and independent or dependent (cooperative). In that case, there will be intrinsic binding affinities and enthalpies for each site, and a cooperativity constant and a cooperativity enthalpy[19-22]. The molecular basis for the cooperativity may be rooted in a direct steric effect between bound titrant molecules, or in an indirect long-range effect caused by a conformational change in the titrand molecule. The complexity is further increased if the number of binding sites is larger, where the topology of the titrand molecule with several binding sites must be defined in terms of geometric layout of the sites and inter-site contacts within the model, giving rise to the different combinations of cooperativity constants and enthalpies. The modification of the basic experimental protocol is

straightforward, just requiring an increase of the titrant concentration in the syringe beyond the 10-/20-fold factor with regard to the titrand concentration. The increase is proportional to the number of binding sites on the titrand. The main difficulty for these experiments lies in the data analysis; although it can be done with the commercial software provided by the manufacturer, the interpretation of the estimated parameters is not straightforward. When studying titrand molecules with several binding sites it is advisable to perform reverse titrations, which may strengthen the robustness of the fit and confirm the selected binding model. It is also recommended to perform experiments at different temperatures and different concentrations, because cooperative effects may remain hidden at certain experimental conditions[23-25].

Interaction of a macromolecule with two different ligands. Almost all proteins are capable of interacting with multiple ligands, corresponding to heterotropic cooperativity. Proteins are able to interact with a certain biological partner and possess at least one ionisable group. In fact, heterotropic effects are the molecular basis for the *pH* dependency of the ligand binding affinity. As in the homotropic case, there will be intrinsic binding affinities and enthalpies for each ligand, and a cooperativity constant and enthalpy[26]. Similarly, the molecular basis for the cooperativity may be rooted in a direct steric effect between bound ligand molecules, or in an indirect long-range effect caused by a conformational change in the titrand molecule. Thus, the basic difference between homotropy and heterotropy is the chemical nature of the binding ligands. As in the previous case, the complexity is further increased if the number of binding sites is larger, even coupling homotropic cooperativity with heterotropic cooperativity. The modification of the basic experimental protocol is straightforward, just requiring the pre-mixing of the titrand molecule with one of the binding molecules, normally the secondary ligand, at a sufficiently high concentration, and then performing injections of the primary ligand. The titration can be performed at different concentrations of the secondary ligand in order to evaluate the secondary ligand concentration-dependence of the apparent binding parameters of the primary ligand[27-29]. Appropriate analysis using a quasi-binary model, *i.e.,* analysis of the ternary titrations as if they were binary ones, provides the binding parameters for both secondary and primary ligands[27,28]. Alternatively, a single ternary titration can be analysed employing an exact ternary model from which the cooperativity parameters can be estimated[28,29]. Reversing the definition of the secondary and primary ligands is advisable, because it may improve the robustness of the analysis. The cooperativity effect must be reciprocal: if the binding of a ligand affects the binding affinity another ligand by a certain factor, then binding affinity of the first ligand must be affected by the second ligand to the same extent.

Displacement titrations. Displacement binding represents a special type of ternary titrations in which a pre-bound ligand is displaced by another injected ligand in a form of maximal negative heterotropic cooperativity. Both ligands occupy the same ligand binding site or a very close and sterically excluding binding site. This type of experiments has been employed for the determination of very tight (K_d < 1 nM) and very weak (K_d > 100 μM) binding affinities[30-35], without the need for modifying the experimental conditions as done some studies[36,37]. A special setup for ternary titrations has made possible to study protein-metal ion interactions avoiding lengthy and risky dialysis procedures (protein precipitation or adsorption onto dialysis membrane) for removing the metal ion from the protein during sample preparation: either titrating a chelating agent (*e.g.,* EDTA or EGTA) solution into a solution of protein with a slight excess of metal, or titrating a metal solution into a solution of protein with a slight excess of chelating agent, allows estimating the binding parameters for the protein-metal ion interaction[38-40].

Competition titrations. These are another type of ternary titrations where there is simultaneous competition of two binding partners to a common macromolecule. This is a variation of the ternary titration in which no pre-mixing of any of the ligands with the macromolecule is done. This protocol has been employed for determination of high affinities for very insoluble compounds[41] or for determining differential affinities in a mix of stereoisomers of a chemical compound[42].

Micellization of amphipathic substances. Micelle formation can be studied and the critical micelle concentration (CMC), the micellization enthalpy, and the number of molecules per micelle can all be determined[43,44]. Further, assays can be designed to monitor the reconstitution of membrane-protein assemblies[45].

Enzymatic activity. Enzyme activity can be studied by employing a step-wise addition of substrate into a very dilute enzyme solution (applying a first-order kinetic approximation) in which a stepped thermogram is obtained, or employing a single-injection protocol in which a quasi-continuous thermal power curve is obtained. In both cases, the direct output (reaction thermal power) can be processed to be converted into a Michaelis-Menten curve from which the enzymatic parameters k_{cat} and K_M can be estimated[46-50]. An outstanding advantage when monitoring enzymatic by ITC is that there is no need for using unnaturally-modified substrates or coupled enzymatic reactions, since virtually any catalytic process will have a non-zero enthalpy of reaction (or experimental conditions can be slightly modified to get a non-zero enthalpy change). In addition, diluted cell extracts and other optically active samples can be tested with no major complications.

Single injection method. An additional development consists of substituting the series of small injections of titrant by a single injection equivalent to the total volume[51]. The advantage of this modified procedure is that the experimental time is considerably reduced, and the thermogram can be converted directly into a quasi-continuous interaction isotherm with very high time resolution. This improves the estimation of the binding affinity and the binding enthalpy. However, it may be argued that the calculation of the effective concentration of reactants in the sample cell could be somewhat uncertain.

Other protocols. Not necessarily requiring a modified protocol, but the study of adsorption of biomolecules on nanoparticles deserves special attention because of the biotechnological and biomedical interest of biofunctionalization[52-54], as well the study of supramolecular chemistry and encapsulation of biomolecules in nanopolymers for drug delivery[55,56].

Flow chart for ITC data analysis

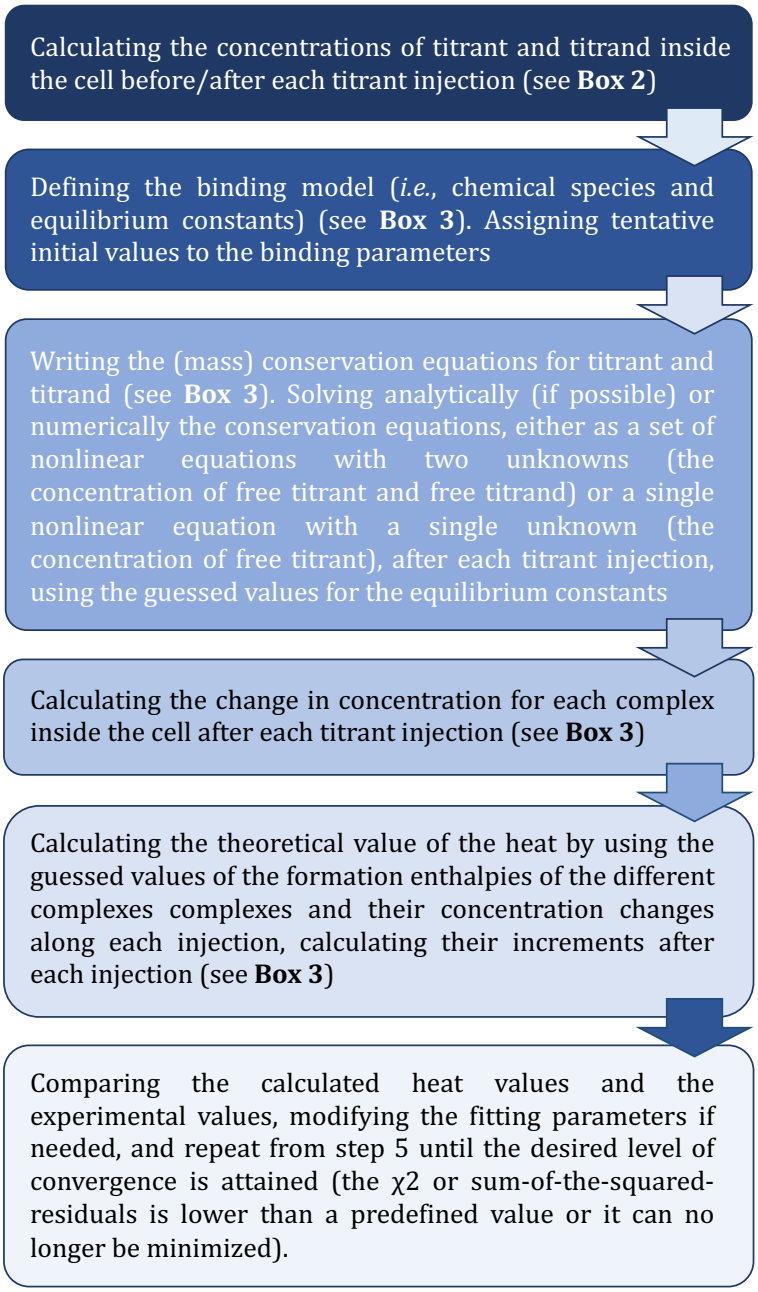

Is the Wiseman isotherm an appropriate representation?

Least-squares regression data analysis for parameter estimation imposes two main assumptions conditioning the processing and representation of experimental data: 1) x-variable must be an independent variable with negligible error; and 2) y-variable must be normally distributed. Because of this many linearization representations such as the Lineweaver-Burk in enzymology or

the Scatchard plot in binding) should not be employed for parameter estimation, and only used for visual depiction purposes.

Similarly, it could be argued that the Wiseman isotherm does not comply with these basic assumptions for least-squares fitting analysis, in particular the assumption that the x-variable is unaffected by experimental error. On the other hand, the main advantage of the Wiseman isotherm is that titrations performed with different instruments (different cell or syringe volumes) or with different experimental settings (injection volumes, number of injections, etc.) can be easily superimposed and compared. If there are no errors, the same Wiseman isotherm should be obtained even changing the experimental setup. Another additional advantage is that certain geometric features of the isotherm are directly linked to the binding parameters and, in principle, the binding parameters could be obtained with no need of a nonlinear fitting analysis[57]. It can be noted that the original Wiseman isotherm was developed considering an analytical derivative ($dQ/d[X]_T$ *vs* $[X]_T/[M]_T$), instead of the quotient of finite increments. Nevertheless, provided that the volume of injection is sufficiently smaller than the cell volume, both formulations are equivalent. Very recently, a new formalism has provided the mathematical basis to reach an agreement between both alternative views[58].

In summary, though the Wiseman isotherm is not strictly an optimal representation, it is a convenient one.

Protein sample quality

Molecular interactions comprising proteins are amongst the most studied and relevant to understand biological systems and for drug discovery. The quality of protein samples is key for the reliability and reproducibility of the data collected with ITC in the scope of the characterization of binding events and macromolecular assemblies involving proteins.

The need for a systematic and comprehensive quality control (QC) of protein samples has prompted the recent publication of guidelines for the quality assessment and sample improvement[59-61] (for updated versions see https://p4eu.org/protein-quality-standard-pqs/ and https://arbre-mobieu.eu/guidelines-on-protein-quality-control/). As expected, the implementation of QC has been shown to improve data quality and reproducibility[62].

These guidelines consist of three parts:

1. Minimal information to provide in publications
    a. Protein name and sequence (database accession number), source of DNA (species) and cloning strategy
    b. Expression and purification details
    c. Method used for measuring protein concentration and storage conditions
2. Minimal quality control parameters
    a. Identity (assessed by intact protein mass and peptide mass fingerprinting by MS)
    b. Purity (assessed by SDS-PAGE, papillary Electrophoresis and/or RP-HPLC)
    c. Mass and size homogeneity (assessed by SEC, DLS, SEC-MALS or AUC)
3. Extended quality control parameters
    a. Folding state (assessed by circular dichroism, NMR, FTIR)
    b. Stability (assessed by DSC, thermal shift, nano-DSF)
    c. Non protein contaminants (*e.g.,* nucleic acids assessed by UV spectrophotometry)

d. Function (*e.g.,* activity of an enzyme)

QC should be performed on every protein and for all batches of protein used in ITC experiments. An extended set of QC parameters may also be applied depending on the protein, its properties, and its availability. QC data inform the decision whether samples are suitable for ITC and other downstream applications or if further optimisation of protein purification, formulation, or storage conditions are required[63].

Calorimetry measures heat, but… what if enthalpy is zero?

The success of ITC for determining affinities relies on the ability to measure the heat of the binding reaction. Then, what happens when the observed binding enthalpy is close to zero? It may be possible to confuse a zero-enthalpy interaction with a case of no interaction. Fortunately, if the enthalpy of binding is zero at T_H, even though ΔG shows low sensitivity to temperature, its two temperature derivatives, ΔH and ΔS:

$$\frac{\partial \Delta G/T}{\partial 1/T} = \Delta H$$
$$\frac{\partial \Delta G}{\partial T} = -\Delta S$$

are strongly dependent on temperature:

$$\frac{\partial \Delta H}{\partial T} = T\frac{\partial \Delta S}{\partial T} = \Delta C_P$$
$$\Delta H(T) = \Delta H(T_0) + \Delta C_P(T - T_0)$$
$$\Delta S(T) = \Delta S(T_0) + \Delta C_P \ln\frac{T}{T_0}$$

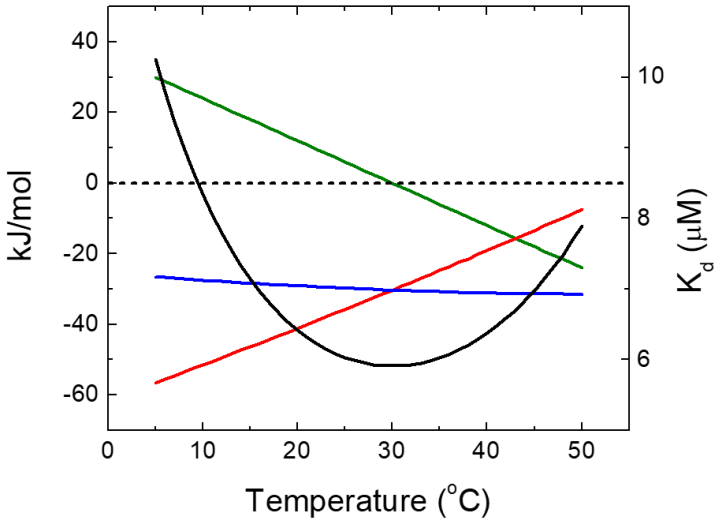

In the previous Figure, the temperature dependency of the binding parameters for a particular interaction with the following parameters has been plotted: ΔH(25 °C) = 6 kJ/mol, $-T\Delta S$(25 °C) = –36 kJ/mol, and ΔC_P = –1.2 kJ/mol. Along the 45 °C temperature range, the Gibbs energy (blue) undergoes just a –5 kJ/mol variation, but the enthalpy (green) and the entropic contribution (red)

show a ~50 kJ/mol variation. According to its direct connection with the Gibbs energy, the dissociation constant also undergoes minor changes (less than 2-fold change).

Therefore, performing titrations at different temperatures (and if ΔC_P is non-zero), the binding affinity and enthalpy can be determined in the vicinity of T_H, and the binding and enthalpy of binding at T_H can be calculated by interpolation. Additional experiment might involve making changes in *pH* or selecting another buffer molecule in order (benefitting in this case from the contribution of buffer ionisation to the overall enthalpy) to make the observed enthalpy different from zero.

References

1. Christensen, J. J., Johnston, H. D. & Izatt, R. M. An isothermal titration calorimeter. *Rev. Sci. Instrum.* **39**, 1356–1359 (1968).

2. Christensen, J. J., Gardner, J. W., Eatough, D. J., Izatt, R. M., Watts, P. J., & Hart, R. M. An isothermal titration microcalorimeter. *Rev. Sci. Instrum.* **44**, 481–484 (1973).

3. Spokane, R. B. & Gill, S. J. Titration microcalorimeter using nanomolar quantities of reactants. *Rev. Sci. Instrum.* **52**, 1728–1733 (1981).

4. McKinnon, I. R., Fall, L., Parody-Morreale, A. & Gill, S. J. A twin titration microcalorimeter for the study of biochemical reactions. *Anal. Biochem.* **139**, 134–139 (1984).

5. Wiseman, T., Williston, S., Brandts, J. F. & Lin, L.-N. Rapid measurement of binding constants and heats of binding using a new titration calorimeter. *Anal. Biochem.* **179**, 131–137 (1989).

6. Freire, E., Mayorga, O. L., & Straume, M. Isothermal titration calorimetry. *Anal. Chem.* **62**, 950A–959A (1990).

7. El Harrous, M., Gill, S. J. & Parody-Morreale, A. Description of a new Gill titration calorimeter for the study of biochemical reactions. I: assembly and basic response of the instrument. *Meas. Sci. Technol.* **5**, 1065 (1994).

8. Velazquez-Campoy, A., Lopez-Mayorga, O., & Cabrerizo-Vilchez, M. A. Development of an isothermal titration microcalorimetric system with digital control and dynamic power Peltier compensation. I. Description and basic performance. *Rev. Sci. Instrum.* **71**, 1824 (2000).

9. Plotnikov, V. V., Brandts, J. M., Lin, L.-N. & Brandts, J. F. A new ultrasensitive scanning calorimeter. *Anal. Biochem.* **250**, 237–244 (1997).

10. Keller, S., Vargas, C., Zhao, H., Piszczek, G., Brautigam, C. A. & Schuck, P. High-precision isothermal titration calorimetry with automated peak-shape analysis. *Anal. Chem.* **84**, 5066-5073 (2012).

11. Scheuermann, T. H., Brautigam, C. A. High-precision, automated integration of multiple isothermal titration calorimetric thermograms: new features of NITPIC. *Methods* **76**, 87–98 (2015).

12. Brautigam, C. A., Zhao, H., Vargas, C., Keller, S. & Schuck, P. Integration and global analysis of isothermal titration calorimetry data for studying macromolecular interactions. *Nat. Protoc.* **11**, 882-894 (2016).

13. Piñeiro, A., Muñoz, E., Sabin, J., Costas, M., Bastos, M., Velazquez-Campoy, A., Garrido, P. F., Dumas, P., Ennifar, E., Garcia-Rio, L., Rial, J., Perez. D., Fraga, P., Rodriguez, A. & Cotelo, C. AFFINImeter: A software to analyze molecular recognition processes from experimental data. *Anal. Biochem.* **577**, 117–134 (2019).

14. Muñoz, E., Sabin, J., Rial, J., Perez, D., Ennifar, E., Dumas, P. & Piñeiro, A. Thermodynamic and kinetic analysis of isothermal titration calorimetry experiments by using kinitc in AFFINImeter. *Methods Mol. Biol.* **1964**, 225–239 (2019).

15. Burrows, S. D., Doyle, M. L., Murphy, K. P., Franklin, S. G., White, J. R., Brooks, I., McNulty, D. E., Scott, M. O., Knutson, J. R., Porter, D., Young, P. R. & Hensley, P. Determination of the monomer-dimer equilibrium of interleukin-8 reveals it is a monomer at physiological concentrations. *Biochemistry* **33**, 12741-12745 (1994).

16. Luke, K., Apiyo, D. & Wittung-Stafshede, P. Dissecting homo-heptamer thermodynamics by isothermal titration calorimetry: entropy-driven assembly of co-chaperonin protein 10. *Biophys. J.* **89**, 3332-3336 (2005).

17. Bello, M., Perez-Hernandez, G., Fernandez-Velasco, D. A., Arreguin-Espinosa, R. & Garcia-Hernandez, E. Energetics of protein homodimerization: effects of water sequestering on the formation of beta-lactoglobulin dimer. *Proteins* **70**, 1475–1487 (2008).

18. Velazquez-Campoy, A., Leavitt, S.A. & Freire, E. Characterization of protein-protein interactions by isothermal titration calorimetry. *Methods Mol. Biol.* **1278**, 183–204 (2015).

19. Wyman, J. & Gill, S. J. Binding and linkage: functional chemistry of biological macromolecules. Mill Valley: University Science Books (1990).

20. Freire, E., Schön, A. & Velazquez-Campoy, A. Isothermal titration calorimetry: general formalism using binding polynomials. *Methods Enzymol.* **455**, 127–155 (2009).

21. Vega, S., Abian, O. & Velazquez-Campoy, A. A unified framework based on the binding polynomial for characterizing biological systems by isothermal titration calorimetry. *Methods* **76**, 99–115 (2015).

22. Vega, S., Abian, O. & Velazquez-Campoy, A. Handling complexity in biological interactions. *J. Thermal Anal. Calorim.* **138**, 3229–3248 (2019).

23. Freiburger, L. A., Auclair, K. & Mittermaier, A. K. Elucidating protein binding mechanisms by variable-c ITC. *Chembiochem* **10**, 2871-2873 (2009).

24. Claveria-Gimeno, R., Velazquez-Campoy, A. & Pey, A. L. Thermodynamics of cooperative binding of FAD to human NQO1: Implications to understanding cofactor-dependent function and stability of the flavoproteome. *Arch. Biochem. Biophys.* **636**, 17-27 (2017).

25. Felix, J., Weinhäupl, K., Chipot, C., Dehez, F., Hessel, A., Gauto, D. F., Morlot, C., Abian, O., Gutsche, I., Velazquez-Campoy, A., Schanda, P. & Fraga, H. Mechanism of the allosteric activation of the ClpP protease machinery by substrates and active-site inhibitors. *Sci. Adv.* **5**, eaaw3818 (2019).

26. Vega, S., Abian, O. & Velazquez-Campoy, A. A unified framework based on the binding polynomial for characterizing biological systems by isothermal titration calorimetry. *Methods* **76**, 99–115 (2015).

27. Du, W., Liu, W. S., Payne, D. J. & Doyle, M. L. Synergistic inhibitor binding to Streptococcus pneumoniae 5-enolpyruvylshikimate-3-phosphate synthase with both monovalent cations and substrate. *Biochemistry* **39**, 10140-10146 (2000).

28. Velazquez-Campoy, A., Goñi, G., Peregrina. J. R. & Medina, M. Exact analysis of heterotropic interactions in proteins: Characterization of cooperative ligand binding by isothermal titration calorimetry. *Biophys. J.* **91**, 1887–904 (2006).

29. Houtman, J. C., Brown, P. H., Bowden, B., Yamaguchi, H., Appella, E., Samelson, L. E. & Schuck, P. Studying multisite binary and ternary protein interactions by global analysis of isothermal titration calorimetry data in SEDPHAT: application to adaptor protein complexes in cell signaling. *Protein Sci.* **16**, 30–42 (2007).

30. Sigurskjold, B. W. Exact analysis of competition ligand binding by displacement isothermal titration calorimetry. *Anal. Biochem.* **277**, 260-266 (2000).

31. Zhang, Y. L. & Zhang Z. Y. Low-affinity binding determined by titration calorimetry using a high-affinity coupling ligand: a thermodynamic study of ligand binding to protein tyrosine phosphatase 1B. *Anal. Biochem,* **261**, 139–148 (1998).

32. Bradshaw, J. M., Mitaxov, V. & Waksman, G. Investigation of phosphotyrosine recognition by the SH2 domain of the Src kinase. *J. Mol. Biol.* **293**, 971–985 (1999).

33. Ohtaka, H., Velazquez-Campoy, A., Xie, D. & Freire, E. Overcoming drug resistance in HIV-1 chemotherapy: the binding thermodynamics of Amprenavir and TMC-126 to wild-type and drug-resistant mutants of the HIV-1 protease. *Protein Sci.* **11**, 1908–1916 (2002).

34. Velazquez Campoy, A. & Freire, E. ITC in the post-genomic era...? Priceless. *Biophys. Chem.* **115**, 115-124 (2005).

35. Velazquez-Campoy, A. & Freire, E. Isothermal titration calorimetry to determine association constants for high-affinity ligands. *Nat. Protoc.* **1**, 186-191 (2006).

36. Doyle, M. L., Louie, G., Dal Monte, P. R. & Sokoloski, T. D. Tight binding affinities determined from thermodynamic linkage to protons by titration calorimetry. *Methods Enzymol.* **259**, 183-194 (1995).

37. Doyle, M.L. & Hensley, P. Tight ligand binding affinities determined from thermodynamic linkage to temperature by titration calorimetry. *Methods Enzymol.* **295**, 88-99 (1998).

38. Nielsen, A. D., Fuglsang, C. C. & Westh, P. Isothermal titration calorimetric procedure to determine protein-metal ion binding parameters in the presence of excess metal ion or chelator. *Anal. Biochem.* **314**, 227–234 (2003).

39. Abian, O., Neira, J. L., Velazquez-Campoy, A. Thermodynamics of zinc binding to hepatitis C virus NS3 protease: a folding by binding event. *Proteins* **77**, 624–636 (2009).

40. Fraga, H., Papaleo, E., Vega, S., Velazquez-Campoy, A. & Ventura, S. Zinc induced folding is essential for TIM15 activity as an mtHsp70 chaperone. *Biochim. Biophys. Acta.* **1830**, 2139–2149 (2013).

41. Krainer, G., Broecker, J., Vargas, C., Fanghänel, J. & Keller, S. Quantifying high-affinity binding of hydrophobic ligands by isothermal titration calorimetry. *Anal. Chem.* **84**, 10715–10722 (2012).

42. Fokkens, J. & Klebe, G. A simple protocol to estimate differences in protein binding affinity for enantiomers without prior resolution of racemates. *Angew. Chem. Int. Ed. Engl.* **45**, 985-989 (2006).

43. Olesen, N. E., Holm, R. & Westh, P. Determination of the aggregation number for micelles by isothermal titration calorimetry. *Thermochim. Acta* **588**, 28–37 (2014).

44. Tso, S. C., Mahler, F., Höring, J., Keller, S. & Brautigam, C. A. Fast and robust quantification of detergent micellization thermodynamics from isothermal titration calorimetry. *Anal. Chem.* **92**, 1154–1161 (2019).

45. Jahnke, N., Krylova, O. O., Hoomann, T., Vargas, C., Fiedler, S., Pohl, P. & Keller, S. Real-time monitoring of membrane-protein reconstitution by isothermal titration calorimetry. *Anal Chem.* **86**, 920-927 (2014).

46. Todd, M. J. & Gomez, J. Enzyme kinetics determined using calorimetry: a general assay for enzyme activity? *Anal. Biochem.* **296**, 179-187 (2001).

47. Transtrum, M. K., Hansen, L. D. & Quinn, C. Enzyme kinetics determined by single-injection isothermal titration calorimetry. *Methods* **76**, 194-200 (2015).

48. Hansen, L. D., Transtrum, M. K., Quinn, C. & Demarse, N. Enzyme-catalyzed and binding reaction kinetics determined by titration calorimetry. *Biochim. Biophys. Acta.* **1860**, 957-966 (2016).

49. Zambelli, B. Characterization of enzymatic reactions using ITC. *Methods Mol. Biol.* **1964**, 251–266 (2019).

50. Wang, Y., Wang, G., Moitessier, N. & Mittermaier, A. K. Enzyme kinetics by isothermal titration calorimetry: allostery, inhibition, and dynamics. *Front. Mol. Biosci.* **7**, 583826 (2020).

51. Markova, N. & Hallén, D. The development of a continuous isothermal titration calorimetric method for equilibrium studies. *Anal. Biochem.* **331**, 77–88 (2004).

52. Crowe, M. C. & Campbell, C. T. Adsorption microcalorimetry: recent advances in instrumentation and application. *Annu. Rev. Anal. Chem.* **4**, 41–58 (2011).

53. Prozeller, D., Morsbach, S., Landfester, K. Isothermal titration calorimetry as a complementary method for investigating nanoparticle–protein interactions. *Nanoscale* **11**, 19265–19273 (2019).

54. Guyon, L., Groo, A. C. & Malzert-Fréon, A. Relevant physicochemical methods to functionalize, purify, and characterize surface-decorated lipid-based nanocarriers. *Mol. Pharm.* **18**, 44–64 (2021).

55. Arnaud, A. & Bouteiller, L. Isothermal titration calorimetry of supramolecular polymers. *Langmuir* **20**, 6858–6863 (2004).

56. Bouchemal, K. New challenges for pharmaceutical formulations and drug delivery systems characterization using isothermal titration calorimetry. *Drug Discov. Today* **13**, 960-972 (2008).

57. Velazquez-Campoy, A. Geometric features of the Wiseman isotherm in isothermal titration calorimetry. *J. Therm. Anal. Calorim.* **122**, 1477–1483 (2015).

58. Dumas, P. Isothermal titration calorimetry in the single-injection mode with imperfect mixing. *Eur. Biophys. J.* **51**, 77–84 (2022).

59. Lebendiker, M., Danieli, T. & de Marco, A. The Trip Adviser guide to the protein science world: a proposal to improve the awareness concerning the quality of recombinant proteins. *BMC Res Notes* **7**, 585 (2014).

60. Raynal, B., Lenormand, P., Baron, B., Hoos, S. & England, P. Quality assessment and optimization of purified protein samples: why and how? *Microb. Cell Fact.* **13**, 180 (2014).

61. de Marco, A., Berrow, N., Lebendiker, M., Garcia-Alai, M., Knauer, S. H., Lopez-Mendez, B., Matagne, A., Parret, A., Remans, K., Uebel, S. & Raynal B. Quality control of protein reagents for the improvement of research data reproducibility. *Nat. Commun*. **12**, 2795 (2021).

62. Berrow, N., de Marco, A., Lebendiker, M., Garcia-Alai, M., Knauer, S. H., Lopez-Mendez, B., Matagne, A., Parret, A., Remans, K., Uebel, S. & Raynal, B Quality control of purified proteins to improve data quality and reproducibility: results from a large-scale survey. *Eur. Biophys. J.* **50**, 453–460 (2021).

63. Remans, K., Lebendiker, M., Abreu, C., Maffei, M., Sellathurai, S., May, M. M, Vaněk, O. & de Marco, A. Protein purification strategies must consider downstream applications and individual biological characteristics. *Microb. Cell Fact.* **21**, 52 (2022).